Fluorescent magnetosomes for controlled and repetitive drug release under the application of an alternating magnetic field under conditions of limited temperature increase (

Edouard Alphandéry, Darine Abi Haidar, Olivier Seksek, François Guyot, Imène Chebbi

Fluorescent magnetosomes for controlled and repetitive drug release under the application of an alternating magnetic field under conditions of limited temperature increase (< 2.5 °C).

Edouard Alphandéry[+,⊥,*], *Darine Abi Haidar*[++, +++], *Olivier Seksek*[++], *François Guyot*[+], *Imène Chebbi*[⊥]

[+] Sorbonne Université, Muséum National d'Histoire Naturelle, UMR CNRS 7590, IRD, Institut de Minéralogie, de Physique des Matériaux et de Cosmochimie, IMPMC, 75005 Paris, France

[⊥] Nanobacterie SARL, 36 boulevard Flandrin, 75116, Paris, France.

[++] Laboratoire d'imagerie et modélisation en neurobiologie et cancérologie, UMR 8165 CNRS/IN2P3, Paris-Saclay University, 91405, Orsay, France.

[+++] Paris Diderot University, Sorbonne Paris Cité, F-75013, Paris, France.

*Corresponding author Email address: edouardalphandery@hotmail.com, phone: 0033632697020

ABSTRACT: Therapeutic substances bound to nanoparticles have been shown to dissociate following excitation by various external sources of energies or chemical disturbance, resulting in controllable and efficient antitumor activity. Bioconjugation is used to produce magnetosomes associated with Rhodamine B (RhB), whose fluorescence is partially quenched by the presence of the iron oxide and becomes strongly enhanced when RhB dissociates from the magnetosomes under the application of an alternating magnetic field. This novel approach enables to simultaneously release a RhB model molecule and to monitor such mechanism by fluorescence. The dissociating mechanism of RhB is highlighted by exposing a suspension of fluorescent magnetosomes to an alternating magnetic field, by magnetically isolating the supernate of this suspension, and by showing fluorescence enhancement of the supernate. Furthermore, to approach *in vivo* conditions, fluorescent magnetosomes are mixed with tissue or introduced in mouse brain and exposed to the alternating magnetic field. Most interestingly, the percentages of RhB dissociation measured at the beginning of magnetic excitation ($\Delta R/\delta t$) or 600 seconds afterwards (R_{600s}) are $\Delta R/\delta t \sim 0.13\%$ and $R_{600s} \sim 50\%$ under conditions of limited temperature increases (<2.5 °C), larger values than those of $\Delta R/\delta t \sim 0.02\text{-}0.11\%$ and $R_{600s} \sim 13\%$, estimated at temperatures above 2.5 °C. Furthermore, when magnetic excitations are repeated two to five times, temperature increase becomes undetectable, but RhB dissociation continues to occur up to the fifth magnetic excitation. Since large heating temperatures may be damaging for tissues, this study paves the way towards the development of a safe theranostic dissociating nano-probe operating at low temperature.

KEYWORDS: magnetosomes, magnetotactic bacteria, probe, thermometer, fluorescence, luminescence, nano-thermometry, fluorescent nanoparticles, nanotechnology.

ABREVIATIONS: MCR400: magnetosomes produced by magnetotactic bacteria cultivated in the presence of 400 µM of rhodamine B introduced in the bacterial growth medium followed by magnetosome extraction from these bacteria; MC: magnetosomes produced by magnetotactic bacteria cultivated without rhodamine B introduced in the bacterial growth medium followed by magnetosome extraction from these bacteria; FACS: Fluorescence activated cell sorting; AMF: alternating magnetic field; Ca: calcein acetoxymethyl ester; RhB: rhodamine B

DEFINITION: Magnetosome mineral core: Magnetosomes studied here are composed of an iron oxide mineral core essentially composed of crystallized iron oxide surrounded by a layer containing biological material (LPS, proteins, lipids) and rhodamine B. For a schematic picture of these magnetosomes, see scheme 2.

INTRODUCTION

Antitumor activity can be reached with nanoparticles introduced to tumors and exposed to an external source of energy, either producing a temperature increase, [1-5], or the release and activation of a therapeutic substance, [6]. The first method of treatment is usually designated as magnetic hyperthermia. It led to preclinical efficacy on various cancer types, including prostate, [7], glioblastoma, [8-10], head and neck, [11], melanoma, [12], and to a 6 months increase in survival among patients bearing glioblastoma compared with the standard of care, [13, 14]. It also appears to be safer than conventional thermotherapies such as ultrasounds since it yields antitumor activity at more moderate heating temperatures, *i.e.* 41-46 °C, [15-17], compared with temperatures larger than 60 °C for high intensity ultrasound treatments, [18]. To strengthen safety even more, drugs could be released from nanoparticles under magnetic excitation in the absence of a significant temperature increase. Chemical synthesis methods have been used to fabricate dissociating nano-probes, [19-21], but it appears that they often require high temperatures to reach efficient dissociation, possibly due to the relatively strong bonds between the nanoparticles and the therapeutic substance that can't easily be broken at low temperatures.

In this manuscript, we describe the synthesis method of a dissociating nano-probe operating in conditions of limited temperature increase (< 2.5 °C). This nano-probe is further made fluorescent to monitor the dissociation. For that, we introduce in the growth medium of magnetotactic bacteria a fluorescent substance mimicking a therapeutic agent (RhB), [22], we wait for these bacteria to incorporate RhB in the magnetosomes, and we finally extract fluorescent magnetosomes designated as MCR400 from these bacteria. We show that RhB is sufficiently strongly bound to the magnetosomes to enable MCR400 to maintain their fluorescence following their isolation and re-suspension in water. To examine if MCR400 can be used as intracellular probe, fluorescent magnetosomes are then brought into contact with cancer cells and their internalization, cytotoxicity, and fluorescent properties are studied. The operating mechanism of the MCR400 probe is deciphered by exposing a MCR400 suspension to an

alternating magnetic field (AMF), by magnetically separating from bacterial debris the supernate of this suspension in which RhB has potentially been released, and by measuring its fluorescence intensity. To approach real magnetic hyperthermia treatment conditions, MCR400 are either mixed with brain tissue or introduced in a mouse brain and exposed one to five times to an AMF. MCR400 concentration and environment are varied to modulate the magnitude of temperature increases. The initial rate and quantity of RhB released are deduced from the variation of the MCR400 fluorescence intensity, measured at the beginning of magnetic excitation and 600 seconds afterwards, as a function of various heating temperatures.

RESULTS AND DISCUSSION

Properties of whole fluorescent magnetotactic bacteria. In the absence of a compound that can permeabilize the membrane of gram-negative bacteria such as PEI, it is difficult to introduce fluorescent substances inside such bacteria during their growth, [23]. For this reason, it was usually attempted to stain bacteria with RhB following their amplification. It either yielded very weak fluorescence, [24], or more significant fluorescence, [25], depending on the use (or not) of a specific protocol to bind RhB to bacterial membranes. By using magnetotactic bacteria, we were able to trigger a truly unusual behavior, *i.e.* incorporate RhB in these bacteria by simply adding RhB to their growth medium, which in turn seems to have changed their metabolism since both whole bacteria and magnetosomes became larger in the presence of RhB as explained below. The fluorescence of magnetotactic bacteria cultivated in the presence of 400 µM of RhB was observed by optical microscopy. Whereas whole magnetotactic bacteria cultivated without RhB appeared non-fluorescent under optical microscopy observation, [26], those grown in the presence of 400 µM of RhB displayed a strong intracellular fluorescent signal (Fig. 1). This behavior was further supported by flow cytometer measurements. Indeed, the FL3-H signal, which is proportional to RhB fluorescence, is lower than 10 a.u. for bacteria grown without RhB indicating that the bacteria are non-fluorescent according to a criterion of the flow cytometer. It increases to a value larger than 10 a.u. for magnetotactic bacteria cultivated in the presence of RhB,

yielding 54% of fluorescent bacteria according to this criterion (Fig. 2(a) and table S1). To examine possible changes in bacterial morphologies induced by RhB, we analyzed the cloud of points representing the side scatter height (SSC-H) signal as a function of the forward scatter height (FSC-H) signal. Between bacteria grown in the absence and presence of RhB, Figs. 2(b) and 2(c) show that the FSC-H and SSC-H signals increase from 20-200 a.u. up to 200-10000 a.u. and from 30-300 a.u. up to 200-10000 a.u., respectively. Such behavior may be associated with an increase in size of magnetotactic bacteria and magnetosome chains, [27], when RhB is added to the growth medium. It may arise from the chelation of iron by RhB that could simultaneously increase the amount of iron and RhB introduced in magnetotactic bacteria. On the one hand, chelation could result in enhanced stress applied on these bacteria or to change in their metabolism, which would modify their size, [28]. On the other hand, it could favor the formation of larger magnetosomes or longer magnetosome chains due to more iron introduced in these bacteria, [28, 29]. This behavior is further confirmed by comparing the histograms in size of MC and MCR400 presented in Figs. S2(a) and S2(b) deduced from transmission electron microscopy images of bacteria cultivated in the absence (Fig. S3(a)) or presence (Fig. S3(b)) of RhB.. In the absence of RhB, Fig. S2(a) shows that magnetosome sizes with maximum frequency are 22 nm for small magnetosomes (between 0 and 30 nm) and 40 nm for large magnetosomes (between 30 and 60 nm). In the presence of RhB, these two sizes increase to 30 and 52 nm, respectively (Fig. S2(b))., [29].

Properties of MCR400 extracted from magnetotactic bacteria. For the magnetic hyperthermia treatment of tumor, it is difficult to use whole magnetotactic bacteria, due to the too low magnetosome concentration in a bacterial suspension that does not enable sufficient heat production under AMF application, [30]. To enable their potential further use in magnetic hyperthermia, magnetosomes were therefore extracted from fluorescent magnetotactic bacteria. We first analyzed whether the fluorescence of RhB which was observed in the bacterial cells as underlined in the previous section, was maintained following extraction. The FT-IR spectrum of magnetosomes extracted from fluorescent magnetotactic bacteria is presented in Fig. 3(a). It shows the superposition of two series of peaks. The first series of

peaks is also present in RhB free magnetosomes MC (in blue), *i.e.* amide I at 1650 cm^{-1}, amide II at 1530 cm^{-1}, lipopolysaccharides (LPS) or phospholipids at 1050 cm^{-1} and at 1250 cm^{-1}, maghemite iron oxide at 580 cm^{-1}, Fig. 3(a), [31]. The second series of peaks is due to RhB (in red), *i.e.* peaks at 1700 cm^{-1}, 1600 cm^{-1}, 1475 cm^{-1}, 1250 cm^{-1}, 1175 cm^{-1}, 1125 cm^{-1}, 675 cm^{-1}, Fig. 3(c), [32]. These results suggest that in MCR400, RhB is either adsorbed at magnetosome surface or complexed with magnetosomes, possibly due to the carboxylic acid function of RhB that can interact with the FeOH groups at magnetosome surface, [33]. Further proofs of the association of RhB to the magnetosomes in MCR400 are provided by the absorption spectrum of a MCR400 suspension that displays a shoulder at 550 nm (Fig. 3(d)), a wavelength corresponding to maximum absorption by free RhB (Fig. 3(f)) and to the absence of an absorption signal from MC at this wavelength (Fig. 3(e)). Moreover, the fluorescence spectrum of the MCR400 suspension excited at 405 nm, displays a peak at 569 nm (Fig. 3(g)), which is absent in the spectrum of the MC suspension excited in the same conditions as MCR400 (Fig. 3(h)) and is positioned at a slightly lower wavelength than that of 576 nm observed for free RhB (Fig. 3(i)). This wavelength shift is possibly due to interactions between RhB molecules and the magnetosome surface in MCR400, as previously reported for fluorescent molecules associated to other types of nanoparticles, [34].

Cytotoxicity, fluorescence, and internalization properties of MCR400 in the presence of cancer cells. In a previous study, we showed that MCR400 incubation with Zymozan-activated murine peritoneal macrophages leads to enhanced fluorescence intensity, a behavior which was attributed to the capture of MCR400 by lysosome following their cellular internalization leading to RhB dissociation from the magnetosomes at acidic pH, [35]. To be able to use MCR400 as an intracellular fluorescent probe, MCR400 shall not only maintain a high level of fluorescence but also yield limited cytotoxicity. In this study, MCR400 were therefore incubated with MDA-MB-231 cells during 6 hours in the presence (or not) of Calcein AM. The Calcein AM fluorescence emission intensity (FL1-H), which is proportional to the number of viable cells, [36], was observed to increase from 2 for cells alone to ~

1000 for cells in the presence of Calcein AM both with and without MCR400 (Figure 4(a)), indicating that ~97% of cells are viable following MCR400 incubation (table S1). MCR400 therefore do not induce any significant cytotoxicity towards these cancer cells. This result is consistent with the absence of RhB cytotoxicity below a certain concentration threshold, [37]. Furthermore, between cells alone and cells incubated with MCR400, the fluorescence signal of RhB (FL3-H) and its associated percentage of fluorescent cells increase from 1 to 55 (Fig. 4(b)) and from 0% to 99% (table S1), respectively. Therefore, almost all cancer cells become fluorescent following their incubation with MCR400. Finally, to determine if MCR400 internalize in these cancer cells, two types of epi-fluorescence microscopy images of MCR400 incubated with cancer cells were taken, either in the absence (Fig. 4(c)) or presence (Fig. 4 (d)) of RhB emission. The superposition of Figs. 4 (c) and 4 (d), presented in Fig. 4(e), shows that RhB molecules fluoresce where MDA-MB231 cells are located, which suggests that MCR400 have penetrated inside MDA-MB-231 cells without losing their fluorescence properties. The other possible location of MCR400 at cell surface, which may also be considered by analyzing Fig. 4(d), appears unlikely since Fig. 4(c) doesn't show any magnetosome aggregates at this location. MCR400 enhanced fluorescence intensity following cellular internalization was observed with cancer cells (MDA-MB-231) and macrophages, [38], making this behavior likely to occur for different cell types. We can conclude that MCR400 may be used as intracellular fluorescent probe, which could have potential diagnostic and therapeutic applications both *in vitro* and *in vivo*.

Operating mechanism of the MCR400 probe studied in suspension. We further examined the operating mechanism of the MCR400 probe by suspending MCR400 in water at an iron oxide concentration of 1 mg_{Fe}/mL and by applying an AMF of 25 mT and 198 kHz during 1200 seconds that produced a temperature increase of 7 °C (Fig. 5(a)). This yielded conditions in terms of AMF parameters and temperature that are typical to those reached during magnetic hyperthermia, [15, 16]. During magnetic excitation, Fig. 5(b) shows that the fluorescence intensity of this suspension remains unchanged, possibly due to fluorescence quenching by the iron oxide of the magnetosome mineral core,

which could limit RhB emission, [39]. By contrast, the fluorescence intensity of the supernate of this suspension, which was magnetically separated from the magnetosome mineral cores, increased during the first 100 seconds of the magnetic excitation from 1 to 19 a.u. and then stabilized at 18.5-19.5 a.u. between 100 and 1200 seconds (Fig. 5(b)). Such behavior may not come from the variation of the intrinsic RhB fluorescence, which decreases with increasing temperature, [40]. Instead, it may be due to the dissociation of RhB from the magnetosomes under magnetic excitation, which could lead to fluorescence de-quenching. Furthermore, the emission wavelength, corresponding to the maximum fluorescence intensity for an excitation at 405 nm, is observed to increase from 569 nm for MCR400 to 576 nm for the supernate of MCR400. In fact, RhB molecules may either interact with the magnetosomes in the MCR400 suspension leading to an emission wavelength below that of free RhB or may produce such interactions in the supernate of this suspension due to the diffusion of RhB molecules away from the magnetosomes, yielding for the supernate the same emission wavelength as that of free RhB, (Fig. S4(b)). We have highlighted a mechanism by which RhB molecules initially interact with the iron oxide of the magnetosome mineral, resulting in fluorescence quenching. Following AMF application, RhB molecules are released from the magnetosomes, leading to fluorescence intensity increase, which could also be designated as fluorescence de-quenching. Such mechanism could potentially be used to control the release of a drug under the application of an AMF provided RhB is replaced by a therapeutic substance.

***Ex vivo* release of RhB from magnetosome minerals in the presence of a temperature increase comprised between 2.5 °C and 10 °C.** To complement studies in solution and come closer to the real conditions of treatment, we have introduced 2 µl of a suspension containing 40 or 400 µg of MCR400 at a depth of 1 to 3 mm in a mouse brain extracted from a dead mouse (Scheme 3) that we have exposed to an alternating magnetic field of frequency 200 kHz and strength 25 mT for 30 minutes. Figs. 6(a) and 6(b) show that these conditions yield a temperature increase lying within the range of 2.5-10 °C, a similar temperature increase than that reached in a magnetic hyperthermia treatment, which was previously determined as ~ 3-10 °C from preclinical studies carried out with magnetosomes, [15], [16].

Furthermore, the influence of the position of the excitation/detection fiber on MCR400 fluorescence properties was studied in sample 1 by mixing homogenously 40 µg of MCR400 with brain tissue and by positioning this fiber at different heights of 1 to 3 mm above the tissue. The various fiber heights led to similar values of MCR400 fluorescence intensity (Fig. 7(a)), indicating that the distance between the fiber end and the magnetosome region (Scheme 3) is not an important parameter in this distance range.

Between samples 1 and 2, we increased the amount of MCR400 from 40 µg (sample 1) to 400 µg (sample 2), resulting in enhanced heat production and diffusion outside of the injection volume, two behaviors that compensated each other to yield in both cases a similar value of fluorescence intensity, $\Delta F_{600s} \sim 125$ a.u., and percentage of RhB released from the magnetosomes, $R_{600sec} \sim 12\%$, measured 600 seconds following magnetic excitation (Figs. 6(c) to 6(f)).

Given that after a certain time of magnetic excitation (600 seconds), the fluorescence intensity and percentage of released RhB appear to reach saturation and to become independent of temperature and conditions of excitation, we have examined another parameter, *i.e.* the initial rate of released RhB, $\Delta R/\delta t$, which takes place just after activation of the magnetic excitation. It appears to be larger and less influenced by MCR400 interactions with its surrounding environment than rates of release estimated at later stages, hence possibly being a controllable parameter to trigger a therapeutic activity. Most interestingly, between samples 1 and 2, $\Delta R/\delta t$ increases from 0.02 %/sec. to 0.11 %/sec (Figs. 7(c) and 7(d)). On the one hand, such sharp transition could be due to $\Delta T/\delta t$ increase between samples 1 and 2, reaching a certain threshold value of ~ 0.008-0.12 °C/sec. (Figs. 7(c) and 7(d)). However, this hypothesis seems unlikely since Fig. 7 shows that temperature variations influence rather weekly fluorescence intensity and RhB release. On the other hand, it could come from more brain tissue material surrounding the nanoparticles in sample 1 than in sample 2, which could more strongly prevent efficient RhB diffusion. In fact, in sample 1 brain tissue material could have adsorbed at MCR400 surface or fill MCR400 environment when MCR400 were mixed with tissue, while in sample 2 MCR400 could mainly be surrounded by brain liquid and much less by brain tissue materials as was

observed during MCR400 injection in mouse brain. The optimal conditions for efficient release of RhB from magnetosomes and for the monitoring of such mechanism therefore seem to be an environment that does not prevent RhB diffusion away from the magnetosomes, a sufficiently large initial temperature gradient, and the measurement of fluorescence variations carried out at the beginning of magnetic excitation. For *in vivo* or clinical applications, these results imply that magnetosomes could be used to release a drug provided RhB is replaced by a therapeutic substance. Heat and pharmacological treatments could hence potentially be combined during magnetic hyperthermia by using a drug, which would diffuse away from the magnetosomes and thus be activated following magnetic excitation.

Repetitive *ex vivo* release of RhB from magnetosomes under magnetic excitation in the absence of significant temperature increase (< 2.5 °C). Previous studies have reported antitumor activity when magnetic nanoparticles were mixed with tumor cells or introduced to tumors and exposed to an AMF without inducing any measurable temperature increase, [15]. Such behavior was either explained by mechanical disruption of tumor cells induced by AMF application, [41], or to an indirect mechanism of tumor destruction, possibly involving immune cells, such as natural killer, T cells or polynuclear neutrophils, [15], which could eradicate unheated tumor cells. In order to control such mechanism, an immunogenic substance could be bound to nanoparticles and be progressively released from them under AMF application, as recently suggested for lipopolysaccharide (LPS) dissociating from magnetosomes under magnetic excitation, possibly leading to the activation of the immune system against the tumor, [15]. Most interestingly, such activation could be repeated by re-applying the AMF, [15, 16]. Here, by using RhB as a model molecule that mimics the behavior of a therapeutic substance, we examined if such a substance could repetitively dissociate from the magnetosomes in the absence of any significant temperature increase over several AMF applications. For that, we administered 40 µg of MCR400 at a depth of 3 mm in a mouse brain (Scheme 3) that we exposed to five successive magnetic sessions (MS1 to MS5) during which an AMF of 25 mT and 200 kHz was applied for 30 minutes. Whereas MS1 produced a limited temperature increase of 2.4 °C, MS2 to MS5 did not induce any detectable change in

temperature (Fig. 8(a), Fig. 9(c)), presumably due to magnetosome diffusion away from the exposed area. Most interestingly, in the absence of any detectable temperature increase (MS2 to MS5), although the four different parameters F_{600s}, $\Delta F/\delta t$, R_{600s}, $\Delta R/\delta t$, decreased during increasing number of magnetic sessions (Figs. 9(a) and 9(b)), they remained significant, indicating that RhB could be repetitively released from the magnetosomes and that such release could be monitored by measuring the parameters F_{600s} and $\Delta F/\delta t$. This result differs from previous studies which suggested that significant temperature increase was necessary to trigger drug release from nanoparticles, [42-44]. However, to our knowledge such studies did not consider the change in nanoparticle environment or nanoparticle-nanoparticle interactions with increasing temperature, which could strongly influence and possibly hinder efficient drug release. Our finding is interesting for medical applications since it indicates that efficient drug release could be induced by AMF application in the absence of a detectable temperature increase, hence using safer conditions than the high temperatures usually reported to be required for triggering an efficient release mechanism, which could be damaging towards healthy tissues and dangerous for the patient.

CONCLUSION:

In this study, we describe an original method of fabrication of a theranostic fluorescent nano-probe, in which magnetotactic bacteria are cultivated in the presence of RhB followed by magnetosome extraction from these bacteria, yielding a suspension of MCR400. Magnetosomes thus made are shown to maintain their fluorescence properties following internalization in cancer cells, showing their potential use as intracellular theranostic probes. When a MCR400 suspension is exposed to an AMF, it produces enhanced fluorescence intensity of its supernate, indicating the release of RhB from the magnetosomes. The operation of this probe is further highlighted in conditions that are close to those reached in a magnetic hyperthermia treatment, *i.e.* for 40 µg or 400 µg of MCR400 mixed with tissue or introduced in a mouse brain and exposed to the AMF. Indeed, with increasing duration of the magnetic excitation, they lead to an enhancement of MCR400 fluorescence intensity and hence also of RhB

release. Moreover, we demonstrate that we can control such release mechanism by monitoring it through fluorescent measurements, and by adjusting the parameters of the magnetic excitation, the temperature, as well as MCR400 environment and concentration.

To summarize, we have shown that:

i) It is possible to release a substance from a nano-probe and to monitor the dissociation by fluorescence.

ii) The fluorescence, which is initially quenched by the iron oxide, becomes enhanced following dissociation, making this nano-probe more sensitive than other fluorescent nanoparticles operating under conditions of fluorescence intensity decrease, [45].

iii) Provided the fluorescent substance (Rhodamine B) is replaced by a therapeutic drug, this nano-probe could also be used as a therapeutic drug operating in conditions of limited temperature increase (< 2.5 °C), hence providing safer treatment conditions than conventional thermotherapies working at higher temperatures.

iv) The release of a therapeutic substance could be repeated by re-applying the alternating, hence possibly enabling a therapeutic activity to be triggered repetitively.

The field of drug released from nanoparticles, which is rapidly expanding, [46, 47], should benefit from the new approach presented in this study.

MATERIALS AND METHODS

Culture of magnetotactic bacteria in the presence (or not) of RhB. *Magnetospirillum magneticum* AMB-1 magnetotactic bacteria were obtained from ATCC (ATCC 700274) and grown under micro-aerophile conditions at 30 °C in a growth medium slightly different from the MSGM medium (ATCC medium 1653). In one liter, this medium contained 0.68 g of monobasic potassium phosphate, 0.85 g of sodium succinate, 0.57 g of sodium tartrate, 0.083 g of sodium acetate, 225 µl of 0.2% resazurin, 0.17 g of sodium nitrate, 0.04 g of L-ascorbic acid, 2 ml of a 10 mM iron quinate solution, 10 ml of a solution of Woolf vitamins and 5 ml of a solution of Woolf minerals. While RhB was not introduced in the

bacterial growth medium to synthesize non-fluorescent magnetosomes (MC), 400 µM of RhB were introduced in this medium to synthetize fluorescent magnetosomes (MCR400). The pH of the culture medium was adjusted to 6.85 using a 1M sodium hydroxide solution. The bacteria were collected during the stationary phase and concentrated using a tangential flow filtration column (mPES, 500 kDa) with a flow rate of 950 mL/min and then washed 5 times for 30 minutes with a solution of saline phosphate buffer at pH 7.4 (137 mM NaCl, 2.7 mM KCl, 10 mM $Na2HPO_4$, 1.76 mM $KH2PO_4$). Bacteria were collected by centrifugation at 4000 rpm for 1 hour, the supernatant was removed and the bacteria were re-suspended in 50 mM Tris-HCl buffer solution at pH 7.4 and diluted to yield an optical density of 5 at 600 nm.

Preparation of MC and MCR400 in suspension. Suspensions of magnetotactic bacteria cultivated in the presence (or not) of 400 µM RhB were lysed, magnetosomes were extracted from whole magnetotactic bacteria, bacterial suspensions were sonicated at 30 W at 5 °C during 60 minutes with pulses of 2 sec. and an interval between pulses of 1 sec. Following sonication, magnetosome chains were magnetically isolated from cellular debris using a neodymium magnet. The supernate containing the cellular debris was removed and fluorescent (MCR400) or non-fluorescent (MC) magnetosome chains were washed five times magnetically with a 50 mM Tris-HCl buffer solution at pH 7.4 and then fifteen times with Millipore® water. They were finally re-suspended in Millipore® sterile water to obtain suspensions of MC and MCR400.

Preparation of MC or MCR400 brought into contact with MDA-MB-231 cells. MDA-MB-231 cells were purchased from the American Type Culture Collections (ATCC). They were cultivated in Dulbecco's modified Eagle's medium (DMEM) supplement, which contained 10% fetal calf serum (FCS), 2 mM l-glutamine, 1 mM sodium pyruvate, and 50 U/ml streptomycin, which were purchased from Life Technologies Inc. The cells were then incubated during 6 hours with suspensions of MC and MCR400 at an amount of 63 µg in iron oxide and then studied by flow cytometry or epifluorescence.

Preparation of MC or MCR400 mixed with brain tissue or introduced in a mouse brain. To prepare MC and MCR400 mixed in brain tissue, 2 µl of a MC or MCR400 suspension at a concentration

of 20 mg/mL in iron oxide were mixed homogenously with mouse brain tissue contained in a 2 mm^3 volume. To obtain MC and MCR400 introduced in mouse brains, 2 or 20 µl of a MC or MCR400 suspension at a concentration of 20 mg/mL in iron oxide were introduced at a depth of 1, 2 and 3 mm of a mouse brain extracted from a dead mouse.

Magnetic treatment of MC and MCR400 in suspension, mixed with brain tissue, or introduced in a mouse brain. 300 µl of MC and MCR400 dispersed in suspensions at 3.6 mg/mL in iron oxide were exposed to one magnetic session (MS). MC and MCR400 mixed in brain tissue or introduced in a mouse brain as described above were also exposed to 1 MS. Each MS consisted in the application of an alternating magnetic field (AMF) of 25 mT and 200 kHz for 1200 to 20000 seconds.

Optical microscopy imaging of whole magnetotactic bacteria. 10 µl of a suspension of whole magnetotactic bacteria were deposited on a microscope slide and observed with an inverted phase-contrast microscope (Zeiss Primovert) using an oil immersion objective (100 X, Ph1/0.4) with a LD condenser 0.4 (working distance: 55 mm).

Epifluorescence microscopy of cells brought into contact with MCR400. We imaged MDA-MB-231 cells incubated in the presence of MCR400 to determine if MCR400 were internalized inside these cells. We used the same conditions of incubation as for flow cytometer measurements except that we fixed cells using 5% PFA. We used an epi-fluorescence microscope with an oil immersion objective x64 for optical imaging with/without RhB detection.

Flow cytometer measurements on whole magnetotactic bacteria. We used a flow cytometer to compare the properties of magnetotactic bacteria cultivated in the absence and presence of 400 µM RhB. Before flow cytometer measurements, the bacteria were washed 5 times with deionized water. for each wash, the suspension was placed against a magnet, the supernate was removed, and replaced by deionized water. 500 µl of suspensions containing magnetotactic bacteria cultivated with/without RhB were then mixed with Water Millipore® and introduced into a flow cytometer. The study was carried out using 50 000 bacteria for each condition. The flow cytometer, a FACS-calibur, was equipped with a laser of excitation wavelength 488 nm and enabled to measure various parameters such as size,

granularity and fluorescence of magnetotactic bacteria (or cancer cells see below). These parameters were analyzed simultaneously by means of an optical filter set, which decomposes the light emitted by the fluorochromes and directs each light signal to a different photomultiplier to record it. The detected optical signals were then converted into electrical signals and then stored and analyzed in digital values. This light-matter interaction also led to the diffusion of light by bacteria. These scattering signals were collected along an axial axis (FSC-H: Forward Scattering or axial diffusion) and a lateral axis (SSC-H: Side scattering). The FSC-H signal is proportional to bacterial sizes whereas the SSC-H signal gives information on the intracellular aspect or content of magnetotactic bacteria, *i.e.* on their granularity. The luminescence signal of RhB was also collected through a FL3-H channel at emission wavelengths between 560 nm and 627 nm. According to the flow cytometer specifications, a FL3-H signal lower and larger than the threshold of 10 a.u. corresponds to the absence and presence of RhB fluorescence, respectively. The flow cytometer also estimated the percentage of fluorescent bacteria.

Flow cytometer measurements on MDA-MB231 cells. We used the same flow cytometer as described above to study the viability and fluorescent properties of MDA-MB-231 cancer cells incubated in the presence of MC and MCR400. For that, 500 000 MDA-MB-231 cells contained in a petri dish of 2 mL were incubated during 6 hours with 31.5 µg/mL in iron oxide of MC or MCR400. Then, a cell viability probe, calcein acetoxymethyl ester (Ca), which becomes luminescent in the presence of living cells, was added to the petri dish and the resulting assemblies were collected after trypsinization and centrifugation in tube for flow cytometer measurements. The flow cytometer detected either the fluorescence of Ca (FL1-H) at 530 nm or that of RhB at 585 nm (FL3-H). According to the flow cytometer specifications, FL1-H and FL3-H signals are either lower or larger than a threshold of 10, corresponding to the threshold value above which cells are viable for FL1-H or fluorescent for FL3-H. The flow cytometer also estimated the percentages of viable and fluorescent cells.

FT-IR characterization of MC, MCR400, and RhB. Suspensions at pH 7 containing MC, RhB and MCR400 with a concentration of 1 mg/mL in iron oxide were lyophilized and integrated in a KBr

matrix. Their Fourier Transform infra-red (FT-IR) absorption spectra were recorded using a Nicolet FT-IR model 380 with resolution of 0.5 cm^{-1} and a number of scans of 30.

Transmission electron microscopy of whole bacteria. Electron transmission microscopy images of whole bacteria, MC and MCR400 were obtained with a JEM-2100 from JEOL. For that, 5 µl of a suspension of whole bacteria, MC, and MCR400, were deposited on top of a carbon grid and dried. Size distributions of magnetosomes MC and MCR400, were measured using 300 magnetosomes and plotted in histograms.

Absorption and fluorescence measurements of MC, MCR400, and RhB suspended or mixed in water. The absorption spectra of MC and MCR400 (suspensions containing 40 µg in iron oxide of nanoparticles contained in 1 mL of water) or of RhB (solution containing 4 µg of RhB in 1 mL of water) were recorded between 350 nm and 700 nm using a Varian Cary 3E UV-Vis spectrophotometer. The fluorescence spectra of MC and MCR400 (170 µg in iron oxide of nanoparticles contained in 800µL of water) or of RhB (0.4µg of RhB in 800 µL of water) were recorder on a Aminco-Bowman 2 spectrofluorimeter (Edison, NJ). Fluorescence intensity was recorded between 550 and 650 nm under excitation at 405 nm.

Fluorescence measurements of MCR400 suspended in water in the presence of a magnetic treatment. 1 mg/mL in iron oxide of MCR400 were mixed in 100 µL of water and exposed to one MS, we measured the fluorescence intensity of this suspension and of its supernate, which was magnetically isolated from the magnetosomes using a Neodynium magnet of 0.6 T. We measured the fluorescence intensity of the MCR400 suspension and of its supernate at different times following magnetic excitation (0, 100, 200, 300, 600, 900 or 1200 seconds). Fluorescence intensity was measured at 576 nm for an excitation at 555 nm using a Fluoroskan Ascent (Thermo Scientific) microplate spectrometer.

Fluorescence measurements of MCR400 mixed with brain tissue or introduced in a mouse brain, using a bi-fiber set-up, in the presence of a magnetic treatment. For MCR400 and MC mixed in brain tissue or introduced in mouse brain as described above, samples were excited by a pulsed diode laser emitting at 405 nm with a mean power of 1 mW and a repetition rates of 40 MHz from PicoQuant

(GmbH, Berlin, Germany). A bi-fibered configuration was employed for excitation and collection positioned 3 mm above the surface of the brain or mixed issue. The fibers used for excitation and collection had a core diameter of 200 µm and 365 µm, respectively, with a numerical aperture of 0.22. The spatial resolution was 500 µm. Collected fluorescence signal was sent toward a computer controlled cooled spectrometer (Ocean optics QP600-1-UV-VIS) for spectroscopic analysis. For fluorescence detection, the fiber was positioned 1, 2, or 3 mm, above the lamella for the sample containing MCR400 mixed with brain tissue while it was fixed at a height of 3 mm above the lamella for the sample containing MCR400 introduced in mouse brain at a depth of 1, 2, or 3 mm. In this way, the distance between the fiber end and the center of the samples was the same for a height of 1, 2, or 3 mm in mixed tissue than for a depth of 1, 2, or 3 mm in mouse brain.

Temperature measurements of MCR400 in suspensions mixed with brain tissue or introduced in a mouse brain during a magnetic treatment. For studies in brain tissues and *ex vivo*, spatial temperature distribution in the region containing MCR400 was measured using an Easir 2 thermographic infrared camera positioned 20 cm above the tissues or brain. The plotted temperatures correspond to the highest temperature measured at each time point within the heated surface of ~ 3 mm^2. A microprobe thermocouple (IT-18, Physitemp, Clifton, USA) was inserted inside the magnetosme suspensions and employed for measurements in solution using a Thermes USB (Physitemp) thermometer. The spatial resolutions of the infrared camera and of the thermocouple were 660 µm and 600 µm, respectively.

Temperature parameters $\Delta T_{600sec.}$, $\Delta T/\delta t$, and deduction of magnetosome biodistribution properties from the values of $\Delta T/\delta t$. $\Delta T_{600sec.}$ and $\Delta T/\delta t$ correspond to the temperature increase measured 600 seconds following the beginning of magnetic excitation and to the initial slope of the temperature variation with time, measured at the beginning of magnetic excitation, respectively. For MCR400 mixed in tissue or introduced in mouse brain, we could deduce MCR400 biodistribution properties from the different values $\Delta T/\delta t$ by using the relation between the magnetosome specific absorption rate (SAR), $\Delta T/\delta t$, and the magnetosome concentration, C_{mag}, which is given by:

SAR=$C_v(\Delta T/\delta t)/C_{mag}$, where C_v is the specific heat of water. Assuming that C_v and SAR remain unchanged between the different samples, we deduced that the percentage of MCR400 in the injection volume is proportional to $(\Delta T/\delta t)_2/(\Delta T/\delta t)_1$, where $(\Delta T/\delta t)_2$ and $(\Delta T/\delta t)_1$ are the initial slopes of the temperature variation, measured when MCR400 occupy part or 100% of the injection volume, respectively.

Fluorescence measurement of RhB introduced in mouse brain or mixed with brain tissue, using a bi-fiber set-up, in the absence of magnetic treatment. We followed the same protocols of preparation as for MCR400 mixed with brain tissue or introduced in mouse brain. On the one hand, different quantity of RhB (between 1 ng and 40 ng) were mixed with 2 mm^3 of brain tissue and deposited between a blade and a lamella. On the other hand, 2 µl containing different quantity of RhB dissolved in water (between 1 ng and 100 ng) were introduced at different depth (1, 2, and 3 mm) of a brain extracted from a dead mouse. The fluorescence of the two types of samples was excited and detected using the same bi-fiber set-up and excitation/detection conditions as for MCR400. The fluorescence intensity of free RhB was then plotted as a function of the RhB concentration in these different conditions.

Fluorescence parameters, $\Delta F_{600sec.}$ and $\Delta F/\delta t$. ΔF600sec. corresponds to the fluorescence intensity increase measured 600 seconds following the beginning of magnetic excitation. The measurement time of 600 seconds was selected to be sufficiently long to enable attainment of a stationary state while avoiding fluorescence quenching and possible random MCR400 interactions occurring beyond 600 seconds (Fig. 6(c)). $\Delta F/\delta t$ corresponds to the initial slope of the fluorescence intensity variation with time, measured at the beginning of magnetic excitation, respectively.

Parameters measuring the release of RhB from magnetosomes (R, $R_{600sec.}$ and $\Delta R/\delta t$) for MCR400 mixed with brain tissue or introduced in a mouse brain and exposed to a magnetic treatment. The percentage of RhB released from the magnetosomes was estimated from to the value of the fluorescence intensity of RhB released from the magnetosomes in MCR400 (Fig. 6(c), 6(d), 8(b)), using the formula:

460 $R=100*(Q_{RhBR}/Q_{RhBT})$, where Q_{RhBR} and Q_{RhBT} are the quantities of RhB released from the
461 magnetosomes under magnetic excitation and Q_{RhBT} is the total quantity of RhB associated to the
462 magnetosomes before magnetic excitation. Q_{RhBR} was estimated by measuring $\Delta F = F_{RhBt}-F_{RhBt0}$, where
463 F_{RhBt} and F_{RhBt0} are the fluorescence intensities of RhB during magnetic excitation (time t) and at the
464 beginning of magnetic excitation (t_0) deduced from Figs. 6(c), 6(d) and 8(b). We have then measured
465 and plotted the variation of the fluorescence intensity of free RhB as a function of the quantity of RhB
466 quantity, for RhB mixed with tissue (Fig. S5(a)) or introduced in a mouse brain (Fig. S5(b)). Given that
467 ΔF corresponds to the quantity of RhB dissociated from the magnetosomes, we have deduced Q_{RhBR} by
468 estimating the quantity of RhB corresponding to ΔF values in Figs. S5(a) and S5(b). Q_{RhBT} was
469 estimated by dissolving 40 or 400 µg of MCR400 at pH 0.84. Following this treatment, the fluorescence
470 spectrum of MCR400 shows a peak at 582 nm (Fig. S4(a)), a similar emission wavelength as that of free
471 RhB (Fig. S4(b)), indicating that RhB has dissociated from the magnetosomes. Furthermore, given the
472 value of the maximum fluorescence intensity of this peak of 0.56 a.u. (Fig. S4(a)) as well as the relation
473 between RhB fluorescence intensity and RhB concentration (Fig. S4(c)), we deduced that this treatment
474 induces the dissociation of ~ 750 nmol/L of RhB from the magnetosomes. Q_{RhBT} was then deduced as
475 84 µg and 840 µg for the samples containing 40 µg and 400 µg of MCR400, respectively. $R_{600sec.}$ and
476 $\Delta R/\delta t$ represent the RhB release rate measured 600 seconds following magnetic excitation and the
477 variation of the initial RhB release rate measured at the beginning of magnetic excitation.

478 **Acknowledgment:** We would like to thank the BPI (‘’banque publique d’investissement’’), the region
479 of Paris (‘’Paris Région Entreprise’’), the French Research Tax Credit program (‘’crédit d’impôt
480 recherche’’), the incubator Paris Biotech Santé, the ANRT (CIFRE 2014/0359, CIFRE 2016/0747,
481 CIFRE 2013/0364, CIFRE 2015/976), the Eurostars programs (Nanoneck-2 E9309 and Nanoglioma
482 E11778), the AIR program (‘’aide à l’innovation responsable’’) from the region of Paris (A1401025Q),
483 the ANR (‘’Agence Nationale de la Recherche’’) Méfisto, as well as the Universities Paris 6 and Paris
484 11. Edouard Alphandéry wrote the article and directed the research presented in this article.

REFERENCES:

[1]. Norred, S., E.; Johnson, J., A. Magnetic Resonance-Guided Laser Induced Thermal Therapy for Glioblastoma Multiforme: A Review. *BioMed Research International* **2014**, Article ID 761312.

[2]. Schwarzmaier, H-J., Eickmeyer, F., Von Tempelhoff, W.; Fiedler, V., U.; Niehoff, H., Ulrich, S. D., Yang, Q., Ulrich, F. MR-guided laser-induced interstitial thermotherapy of recurrent glioblastoma multiforme: Preliminary results in 16 patients. *Eur. J. Radiol.* **2006**, 59, 208-215.

[3]. Cetas, T. A Ferrite Core/Metallic Sheath Thermoseed for Interstitial Thermal Therapies. *IEEE transactions on biomedical engineering* **1998**, 45, 68-77.

[4]. Chastellain, M., Petri, A., Gupta, A., Rao, V., Hofmann, H. Superparamagnetic Silica-Iron Oxide Nanocomposites for Application in Hyperthermia. *Advanced Engineering Materials* **2004**, 6, 235-241.

[5]. Giustini, A. J., Petryk, A. A., Cassim, S. M., Tate, J. A., Baker, I., Hoopes, P. J. Magnetic nanoparticle hyperthermia in cancer treatment. *Nano Life* **2010**, 1-23.

[6]. Oliveira, H, Perez-Andrés, E., Thevenot, J., Sandre, O., Berra, E., Lecommandoux, S. Magnetic field triggered drug release from polymersomes for cancer therapeutics. *Journal of controlled released* **2013**, 169, 165-170.

[7]. Johannsen, M., Gneveckow, U., Thiesen, B., Taymoorian, K., Cho, C. B., Waldofner, N., Scholz, R., Jordan, A., Loening, S. A., Wust, P. Thermotherapy of Prostate Cancer Using Magnetic Nanoparticles: Feasibility, Imaging, and Three-Dimensional Temperature Distribution **2007**, 52, 1658-1662.

[8]. Mahmoudi, K., Hadjipanayis, C. G. The application of magnetic nanoparticles of brain tumors. Frontiers in Chemistry **2014**, 2, art 109.

[9]. Verma, J., Lal, S., Van Noorden, C. J. F. Nanoparticles for hyperthermic therapy: synthesis strategies and applications in glioblastioma. *Int. J. Nanomed.* **2014**, 9, 2863-2877.

[10]. Wankhede, M., Bouras, A., Kaluzova, M., Hadjipanayis, C. G. Magnetic nanoparticles: an emerging technology for malignant brain tumor imaging and therapy *Expert Rev Clin Pharmacol.* **2012**, 5, 173-186.

[11]. Zhao, Q., Wang, L., Cheng, R., Mao, L., Arnold, R. D., Howerth, E. W., Chen, Z. G., Platt, S. Magnetic nanoparticle-based hyperthermia for head and neck cancer in mouse models. *Theranostics* **2012**, 2, 113-121.

[12]. Toraya-Brown, S., Sheen, M-R., Zhang, P., Chen, L., Baird, J. R., Demidenko, E., Turk, M. J., Hoopes, Conejo-Garcia, J. R., Fiering, S. Local hyperthermia treatment of tumors induces CD8(+) T cell-mediated resistance against distal and secondary tumors. *Nanomedicine* **2014**, 10, 1273-1285.

[13]. Maier-Hauff, K., Rothe, R., Scholz, R., Gneveckow, U., Wust, P., Thiesen, B., Feussner, A., Von Deimling, A., Waldoefner, N., Felix, R., Jordan, A. Intracranial thermotherapy using magnetic nanoparticles combined with external beam radiotherapy: Results of a feasibility study on patients with glioblastoma multiforme. *J Neurooncol* **2007**, 81, 53–60.

[14]. Maier-Hauff, K., Ulrich, F., Nestler, D., Niehoff, H., Wust, P., Thiesen, B., Orawa, H., Budach, V., Jordan, A. Efficacy and safety of intratumoral thermotherapy using magnetic iron-oxide nanoparticles combined with external beam radiotherapy on patients with recurrent glioblastoma multiforme. *J. Neurooncol.* **2011**, 103, 317-324.

[15]. Alphandéry, E., Idbaih, A., Adam, C, Delattre, J-Y., Schmitt, C., Guyot, F., Chebbi, I. Chains of magnetosomes with controlled endotoxin release and partial tumor occupation induce full destruction of intracranial U87-Luc glioma in mice under the application of an alternating magnetic field. *Journal of Controlled Release* **2017**, 262, 259–272.

[16]. Alphandéry, E., Idbaih, A., Adam, C, Delattre, J-Y., Schmitt, C., Guyot, F., Chebbi, I. Development of non-pyrogenic magnetosome minerals coated with poly-l-lysine leading to full disappearance of intracranial U87-Luc glioblastoma in 100% of treated mice using magnetic hyperthermia. *Biomaterials* **2017**, 141, 210-222.

[17]. Le Fèvre, R., Durand-Dubief, M., Chebbi, I., Mandawala, C., Lagroix, F., Valet, J-P., Idbaih, A., Adam, C., Delattre, J-Y., Schmitt, C., Maake, C., Guyot, F., Alphandéry, E. Enhanced antitumor efficacy of biocompatible magnetosomes for the magnetic hyperthermia treatment of glioblastoma. Theranostics **2017**, 7, 4618-4631.

[18]. Zhou, Y-F. High intensity focused ultrasound in clinical tumor ablation. *World Journal Of Clinical Oncology* **2011**, 10, 8-27.

[19]. Hayashi, K., Nakamura, M., Miki, H., Ozaki, S., Abe, M., Matsumoto, T., Sakamoto, W., Yogo, T., Ishimura, K. Magnetically responsive smart nanoparticles for cancer treatment with a combination of magnetic hyperthermia and remote-control dug release. *Theranostics* **2014**, 4, 834-844.

[20]. Kaewsaneha, C.; Tangboriboonrat, P.; Polpanich, D. and Elaissari, A. Multifunctional Fluorescent-Magnetic Polymeric Colloidal Particles: Preparations and Bioanalytical Applications. *ACS Appl. Mater. Interfaces* **2015**, 7, 23373-23386.

[21]. Laurent, S.; Dutz, S.; Häfeli, U.O. and Mahmoudi, M. Magnetic fluid hyperthermia: Focus on superparamagnetic iron oxide nanoparticles. *Advances in Colloid and Interface Science* **2011**, 166, 8-23.

[22]. Reina, G., Orlanducci, S., Cairone, C., Tamburri, E., Lenti, S., Cianchetta, I., Rossi, M., Terranova, M. L. Rhodamine/Nanodiamand as a System Model for Drug Carrier. *J. nanosci. Nanotechnol.* **2015**, 15, 1022-1029.

[23]. Helander, I., M.; Alakomi, H-L., Latva-Kala, K., Koski, P. Polyethyleneimine is an effective permeabilizer of gram-negative bacteria. *Microbiology* **1997**, 143, 3193-3199.

[24]. Maukonen, J., Mattila-Sandholm, T., Wirtanen, G. Metabolic indicators for assessing bacterial viability in hygiene sampling using cells in suspension and swabbed biofilm. *Lebensm. Wiss. U.-Technol.* **2000**, 33, 225-233.

[25]. Ramachandran, S., Thiyagarajan, S., Raj, G. D., Uma, A. Non-invasive *in vivo* imaging of fluorescence-labeled bacterial distributions in aquatic species. *Inter. J. of Veterinary Science and Medicine* **2017**, 5, 187-195.

[26]. Bazylinski, D.A. and Frankel, R.B. Magnetosome Formation in Prokaryotes. *Nature Reviews Microbiology* **2004**, 2, 217-230.

[27]. Zucker, R. M., Daniel, K. M., Massaro, E. J., Karafas, S. J., Degn, L. L., Boyes, W. K. Detection of silver nanoparticles in cells by flow cytometry using light scatter and far-red fluorescence. Cytometry A. **2013**, 83, 962-972.

[28]. Chien, A-C; Hill, N.S. and Levin, P.A. Cell size control in bacteria. *Current Biology* **2012**, 22, R340-R349.

[29]. Alphandéry E., Amor M., Guyot F., and Chebbi I. The effect of iron-chelating agents on Magnetospirillum magneticum strain AMB-1: stimulated growth and magnetosome production and improved magnetosome heating properties. *Appl. Microbiol. Biotechnol.* **2012**, 96, 663–670.

[30]. Alphandéry, E.; Faure, S.; Raison, L.; Duguet, E.; Howse, P.A. and Bazylinski, D.A. Heat Production by Bacterial Magnetosomes Exposed to an Oscillating Magnetic Field. *Journal of Physical Chemistry C* **2011**, 115, 18-22.

[31]. Li, W., Xiao, F., Su, S., Wanga, D., Yanga, X. Investigation of adsorbtion and photocatalytic activities of in situ cetyltrimethylammonium bromide-modified Bi/BiOCl heterojunction photocatalyst for organic contaminants removal. *RSC Adv.* **2016**, 6, 93309–93317.

575 [32]. Alphandéry, E.; Guyot, F. and Chebbi, I. Preparation of chains of magnetosomes, isolated from
576 Magnetospirillum magneticum strain AMB-1 magnetotactic bacteria, yielding efficient treatment of
577 tumors using magnetic hyperthermia. *International Journal of Pharmaceutics* **2012**, 434, 444-452.

578 [33]. Farag, A. A. M., Yahia, I. S. Structural, absorption and optical dispersion characteristics of
579 rhodamine B thin films prepared by drop casting technique. *Optics Communications* **2010**, 283, 4310-
580 4317.

581 [34]. Boyer, C., Whittaker, M. R., Bulmus, V., Liu, J., Davis, T. P. The design and utility of polymer-
582 stabilized iron-oxide nanoparticles for nanomedicine applications. *NPG Asia Materials* **2010**, 2, 23-30.

583 [35]. Hiderbrand, S.A. and Weissleder, R. Near-infrared fluorescence: application to in vivo
584 molecular imaging. *Current Opinion in Chemical Biology* **2010**, 14, 71-79.

585 [36]. Decherchi, P., Cochard, P., Gauthier, P. Dual staining assessment of Schwann cell viability
586 within whole peripheral nerves using calcein-AM and ethidium homodimer. *J. Neurosci. Methods.*
587 **1997**, 71, 205-213.

588 [37]. Kaji, T., Kawashima, T., Sakamoto, M., Kurashige, Y., Koizumi, F. Inhibitory effect of
589 rhodamine B on the proliferation of huma lip fibroblasts in culture. *Toxicology*. 1991, 68, 11-20.

590 [38]. Alphandéry, E.; Abi Haidar, D.; Seksek O.; Thoreau, M.; Trautmann, A.; Bergovici, N.; Gazeau,
591 F.; Guyot, F.; Chebbi, I. Nanoprobe Synthesized by Magnetotactic Bacteria, Detecting Fluorescence
592 Variations under Dissociation of Rhodamine B from Magnetosomes following Temperature, pH
593 Changes, or the Application of Radiation. *Applied materials and interfaces* **2017**, 9, 36561-36572.

594 [39]. Yu, J., Yang, L., Liang, X., Dong, T., Liu, H. Bare magnetic nanoparticles as fluorescence
595 quenchers for detection of thrombin. *Analyst* **2015**, 140, 4114-4120.

596 [40]. Löw, P., Kim, B., Takama, N., Bergaud, C. High-Spatial-Resolution Surface-Temperature
597 Mapping Using Fluorescent Thermometry. *Small* **2008**, 4, 908-914.

[41]. Goya, G. F., Asin L., Ibarra, M. R. Cell death induced by AC magnetic fields and magnetic nanoparticles: Current state and perspectives. *International Journal of Hyperthermia* **2013**, 29, 810-818.

[42]. Baeza, A., Guisasola, E., Ruiz-Hernandez, E., Vallet-Regi, M. Magnetically triggered multidrug release by hybrid mesoporous silica nanoparticles. *Chem. Mat.* **2012**, 24, 517-524.

[43]. Caetano, B. L., Guilbert, C., Fini, R., Fresnais, J., Pulcinelli, S. H., Ménager, C., Santilli, S. V. Magnetic hyperthermia-induced drug release from ureasil-PEO-γ-Fe2O3 nanocomposities. *RCS Advances* **2016**, 6, 63291-63295.

[44]. Brulé, S., Levy, M., Wilhelm, C., Letourneur, D., Gazeau, F., Ménager, C., Le Visage, C. Doxorubicin release triggered by alginate embedded magnetic nano-heaters: A combined therapy. *Advanced Materials* **2011**, 23, 787-790.

[45]. Homma, M., Takei, Y., Murata, A., Inoue, T., Takeoka, S. A ratiometric fluorescent molecular probe for visualization of mitochondrial temperature in living cells. *Chem. Commun.* **2015**, 51, 6194-6197.

[46]. Hiwale, A. A., Voshavar, C., Dharmalingam, P., Dhayani, A., Mukthavaram, R., Nadella, R., Sunnapu, O., Gandhi, S., Naidu, V. G. M., Chaudhduri, A., Marepally, S., Vemula, P. K. Scaling the effect of hydrophobic chain length on gene transfer properties of di-alkyl, di-hydroxy ethylammonium chloride based cationic amphiphiles. *RCS Advances* **2017**, 7, 25398-25405.

[47]. Kotla, N. G., Chandrasekar, B., Rooney, P., Sivaraman, G., Larranaga, A., Krishna, K. V., Pandit, A., Rochev, Y. Biometric Lipid-Based Nanosystems for Enhanced Dermal Delivery of Drugs and Bioactive Agents. *ACS Biomater. Sci. Eng.* **2017**, 3, 1262-1272.

SCHEME:

Scheme 1: Schematic diagrams showing the steps involved in the preparations of chains of magnetosomes isolated from magnetotactic bacteria and associated to RhB (MCR400). In this preparation, AMB-1 magnetotactic bacteria were first cultivated in a growth medium containing 400 µM of RhB and incubated during 14 days at 30 °C under these conditions. Chains of magnetosomes associated with RhB have then been isolated from these bacteria to yield MCR400.

Scheme 2: Schematic diagrams showing the operating mechanism of the MCR400 probe. Under the application of an alternating magnetic field, RhB dissociates from the magnetosome mineral core yielding enhanced fluorescence intensity and fluorescence wavelength shift.

Scheme 3: (a), Schematic diagram showing the bi-fiber set-up used to excite 2 µl or 20 µl of a MCR400 suspension at a concentration of 20 mg/mL in iron oxide introduced in a brain extracted from a dead mouse at different depth of -1 mm, -2 mm, or – 3 mm, estimated from the mouse brain surface, where the bi-fiber is positioned at 4 mm (∗), 5 mm (∗∗), or 6 mm (∗∗∗) above the center of the region containing the magnetosomes. (b), Schematic diagram showing the bi-fiber set-up used to excite 2 µl of a MCR400 suspension at a concentration of 20 mg/mL in iron oxide mixed with brain tissue, where the center of the bi-fiber is positioned at a distance of 4 mm (1), 5 mm (2), or 6 mm (3) from the center of the tissue.

FIGURES:

Figure 1: Optical image of living AMB-1 magnetotactic bacteria cultivated in the presence of 400 µM of RhB. After 7 days of growth of magnetotactic bacteria in the presence of 400 µM of RhB, an aliquot of 7 µl was taken, deposited on top of a lamella, and observed under optical microscope using an oil objective.

Figure 2: (a), Number of bacteria counted with the flow cytometer as a function of the FL3-H fluorescence signal, measuring RhB fluorescence intensity, for magnetotactic bacteria cultivated in the absence of RhB and in the presence of 400 µM of RhB. The black line plotted between 10^1 and 10^4 delineates the region where bacteria are luminescent. Cloud of points representing the lateral scattering signal (SSC-H) as a function of the forward scattering signal (FSC-H), measured by flow cytometry, of magnetotactic bacteria cultivated in the absence of RhB (b), or in the presence of 400 µM RhB, (c). The values of the SSC-H, FSC-H, and FL3-H signals are expressed in arbitrary units.

Figure 3: FT-IR spectra of chains of magnetosomes extracted from magnetotactic bacteria cultivated in the presence of 400 µM RhB (MCR400), (a), of chains of magnetosomes extracted from magnetotactic bacteria cultivated in the absence of RhB (MC), (b), of free RhB, (c). Absorption spectra of 1 mL of suspensions containing 40 µg of MCR400, (d), 40 µg of MC, (e), 4 µg of free RhB, (f). Fluorescence spectra, recorded for an excitation wavelength of 405 nm, of 800 µL suspensions containing 170 µg of MCR400, (g), 170 µg of MC, (h), 0.4 µg of free RhB, (i).

Figure 4: (a) Number of cells counted with a flow cytometer (FACS-Calibur) as a function of FL1-H signal, measuring Ca fluorescence, for MDA-MB-231 alone (blue histogram), MDA-MB-231 cells in the presence of Ca (blue line), MDA-MB-231 cells in the presence of Ca and fluorescent chains of magnetosomes MCR400 (red line); (b) Number of cells counted with a flow cytometer (FACS-Calibur) as a function of FL3-H signal, measuring RhB fluorescence, for MDA-MB-231 cells in the presence of Ca (Blue line), MDA-MB-231 cells in the presence of Ca and MCR400 (red line); (c), Optical image,

recorded in transmission without rhodamine B fluorescence, of MDA-MB-231 cells incubated with MCR400 during 6 hours. (d), Optical epi-fluorescence image, measuring rhodamine B fluorescence, of MDA-MB-231 cells incubated with MCR400 during 6 hours; (e), Merge of (c) and (d).

Figure 5: (a), for a 100 µL of suspension of MCR400 at an iron oxide concentration of 1 mg/mL exposed to an AMF of 25 mT and 198 kHz during 1200 seconds, variation of temperature of this suspension as a function of time measured using a thermocouple. (b), For the same MCR400 suspension and treatment as in (a), variation of the fluorescence intensity of the MCR400 suspension and of its supernate, which was magnetically from the magnetosomes. The fluorescence was excited at 405 nm. In (b), the initial fluorescence intensity at 0 second is comprised between 0 and 0.4 a.u. (the error bar can't be seen in the graph for this point).

Figure 6: Fluorescence analysis of the MCR400 nano-probe in conditions where the application of an AMF on MCR400 yields a temperature increase of more than 3 °C. For 2 µl of a suspension of MCR400 at a concentration of 20 mg/mL in iron oxide mixed with brain tissue and exposed to an AMF of 200 kHz and 25 mT during 30 minutes, variation of the temperature, (a), fluorescence intensity (c), and percentage of RhB released from the magnetosome mineral core, (e), as a function of time. For 20 µl of a suspension of MCR400 at 20 mg/mL in iron oxide introduced in a mouse brain, variation of the temperature (b), fluorescence intensity, (d), and percentage of RhB released from the magnetosome mineral core, (f), as a function of time. The fluorescence intensity was measured at 580 nm for an excitation at 405 nm. The bi-fiber set-up used for these measurements was such that the distance between the center of the magnetosome regions and the fiber end was 4 mm.

Figure 7: Fluorescence analysis of the MCR400 nano-probe in conditions where the application of an AMF on MCR400 yields a temperature increase of more than 2.5 °C. For 2 µl of MCR400 at 20 mg/mL mixed with brain tissue (40 µg of MCR400 mixed with brain tissue) or 20 µl of MCR400 at 20 mg/mL introduced in a mouse brain (400 µg of MCR400 in brain), fluorescence ($Fluorescence_{600s}$), (a), or

percentage of RhB released from the magnetosome mineral core (R_{600s}), (b), measured 600 seconds after the application of an AMF of 200 kHz and 25 mT, as a function of ΔT_{600s}, where ΔT_{600s} is the difference in temperature between the initial temperature at the beginning of magnetic excitation and the temperature measured after 600 seconds of magnetic excitation. For the same samples and treatments as in (a) and (b), initial slope of the variation of fluorescence with time ($\Delta F/\delta t$), (c), and initial slope of the variation of the percentage of RhB released from the magnetosome mineral core with time ($\Delta R/\delta t$), (d), as a function of the initial slope of the temperature variation with time ($\Delta T/\delta t$). The fluorescence intensity was measured at 580 nm for an excitation at 405 nm. The bi-fiber set-up used for these measurements was such that the distance between the center of the magnetosome regions and the fiber end was 4 mm. In (a) to (d), the dotted lines are guides to the eyes, the numbers 1, 2, 3 represent the positions of the fiber 1, 2, and 3 mm, above the mouse head, while, *, **, and ***, represent the injection depths of 1 mm, 2 mm, and 3 mm (Scheme 3).

Figure 8: Fluorescence analysis of the MCR400 nano-probe in conditions where the application of an AMF on MCR400 yields a temperature increase of less than 2.5 °C. For 2 µl of a suspension of MCR400 at a concentration of 20 mg/mL in iron oxide introduced in a mouse brain at a depth of 3 mm and exposed to several magnetic sessions (MS1 to MS5) during which an AMF of 200 kHz and 25 mT during 30 minutes was applied for 2000 seconds. Variation of temperature, (a), fluorescence intensity (b), and percentage of RhB released from the magnetosomes, (c), as a function of time. The fluorescence intensity was measured at 580 nm for an excitation at 405 nm. The bi-fiber set-up used for these measurements was such that the distance between the center of the magnetosome regions and the fiber end was 4 mm.

Figure 9: MCR400 fluorescence properties for 20 µl of a MCR400 suspension at 20 mg/mL introduced in a mouse brain at a depth of 3 mm and exposed to several magnetic sessions (MS1 to MS5) during which an AMF of 200 kHz and 25 mT during 30 minutes was applied for 2000 seconds. (a), fluorescence intensity measured 600 seconds after magnetic excitation, $F_{600sec.}$, and slope at the origin of

the fluorescence variation with time, $\Delta F/\delta t$ for the various MS. (b), Percentage of released rhodamine B measured 600 seconds following magnetic excitation, $R_{600sec.}$, and slope at the origin of the variation of the percentage of released rhodamine B, $\Delta R/\delta t$, during the various MS. (c), Variation of temperature measured 600 seconds following magnetic excitation, ΔT, and slope at the origin of the temperature variation, $\Delta T/\delta t$, during the various MS.

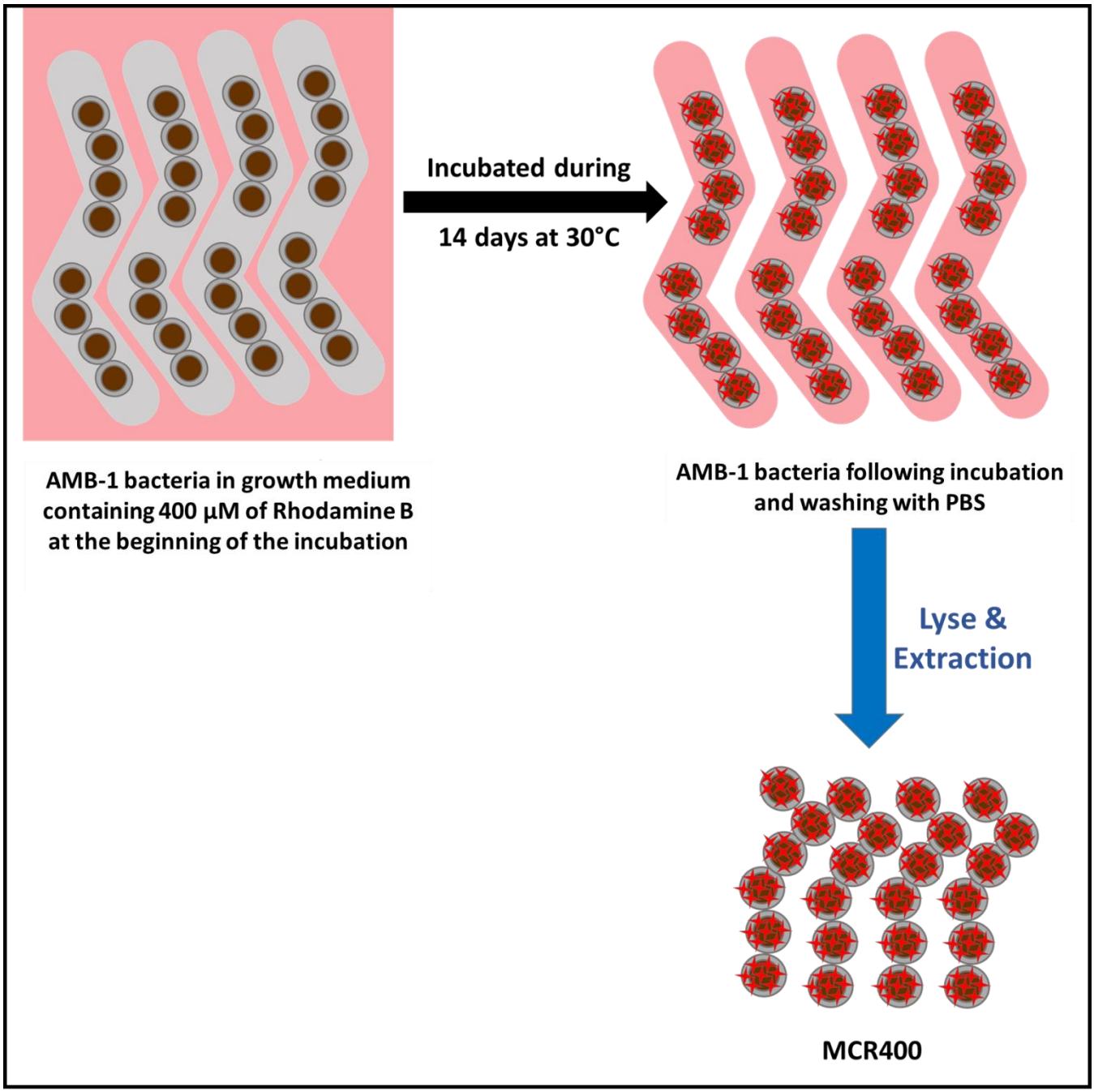
Incubated during
14 days at 30°C
AMB-1 bacteria in growth medium containing 400 µM of Rhodamine B at the beginning of the incubation
AMB-1 bacteria following incubation and washing with PBS
Lyse & Extraction
MCR400

Scheme 1

716

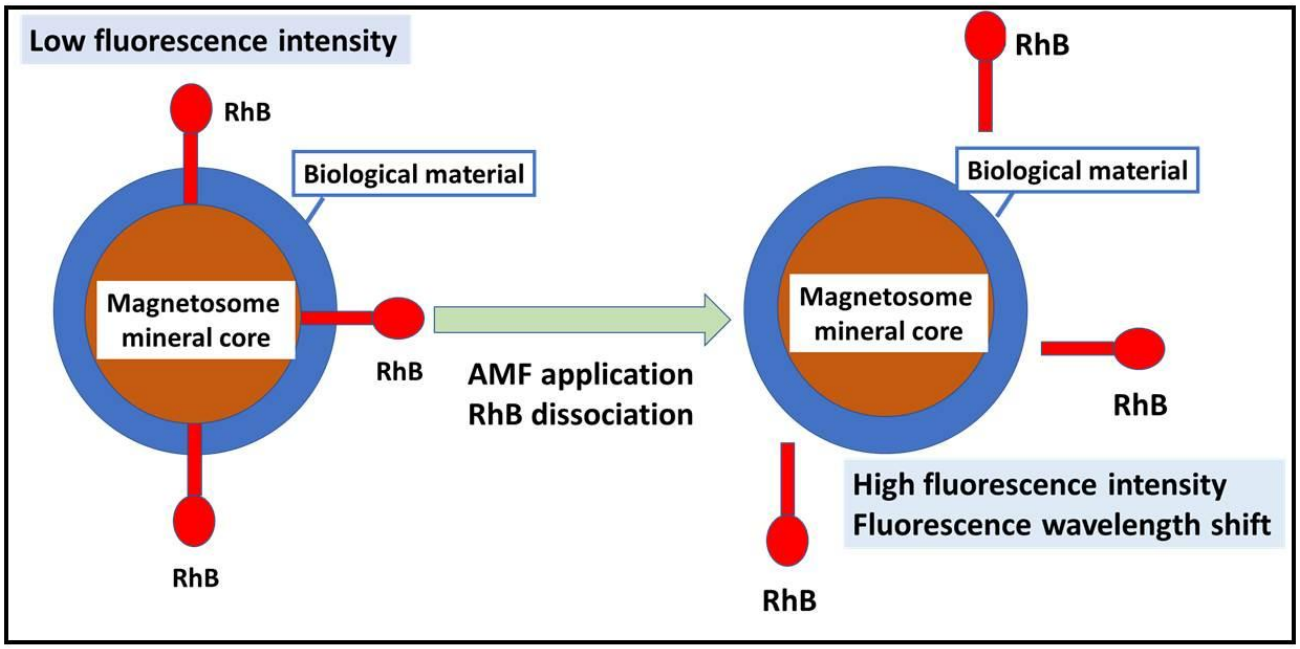
Low fluorescence intensity
RhB
Biological material
Magnetosome mineral core
RhB
RhB
AMF application
RhB dissociation
RhB
Biological material
Magnetosome mineral core
RhB
High fluorescence intensity
Fluorescence wavelength shift
RhB

Scheme 2

717

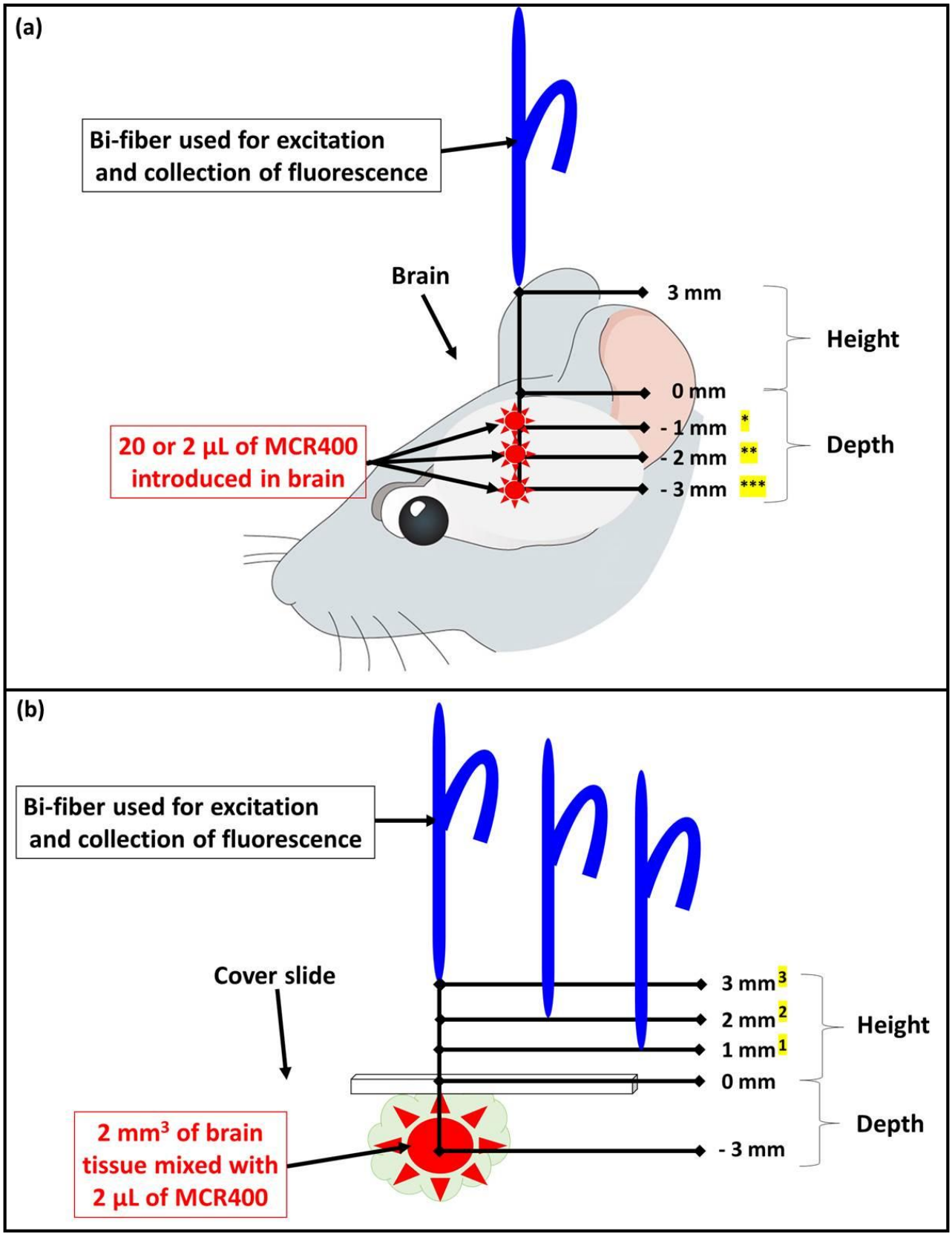
(a)
Bi-fiber used for excitation and collection of fluorescence
Brain
3 mm
Height
0 mm
- 1 mm
- 2 mm
- 3 mm
Depth
20 or 2 µL of MCR400 introduced in brain
(b)
Bi-fiber used for excitation and collection of fluorescence
Cover slide
3 mm
2 mm
1 mm
0 mm
Height
Depth
- 3 mm
2 mm³ of brain tissue mixed with 2 µL of MCR400

Scheme 3

718

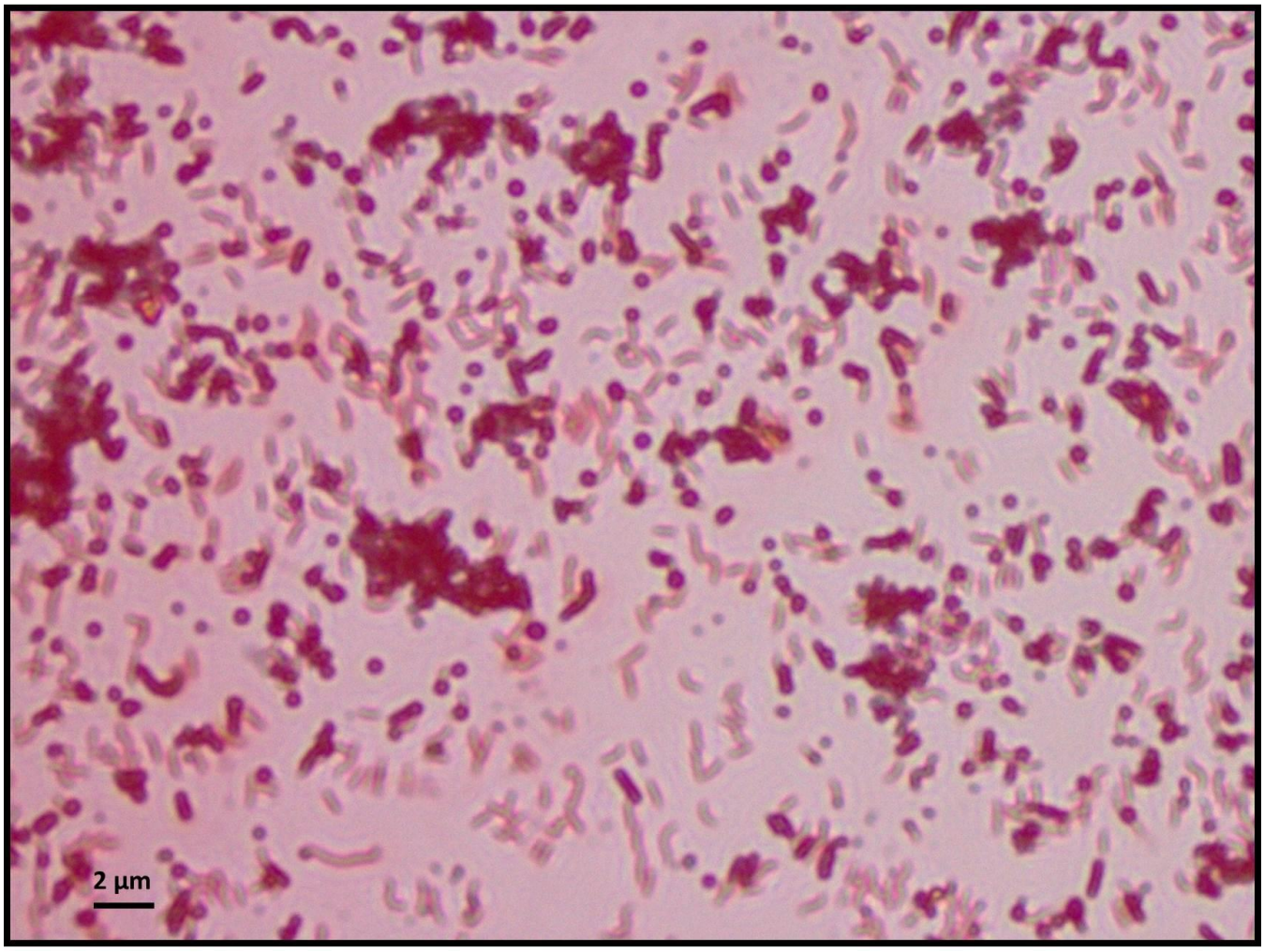

Figure 1

719

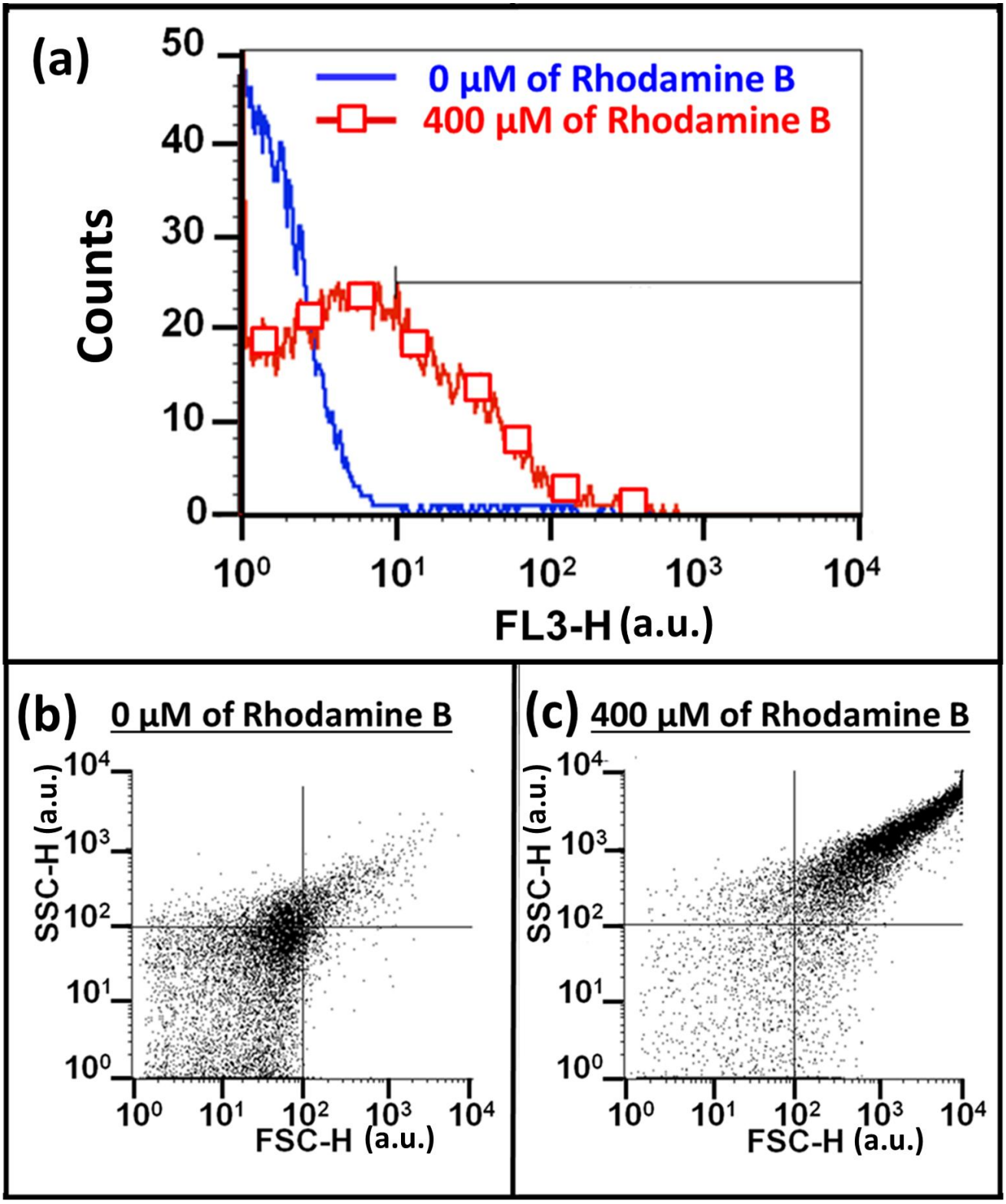
(a)
0 µM of Rhodamine B
400 µM of Rhodamine B
Counts
FL3-H (a.u.)
(b) 0 µM of Rhodamine B
SSC-H (a.u.)
FSC-H (a.u.)
(c) 400 µM of Rhodamine B
SSC-H (a.u.)
FSC-H (a.u.)

Figure 2

720

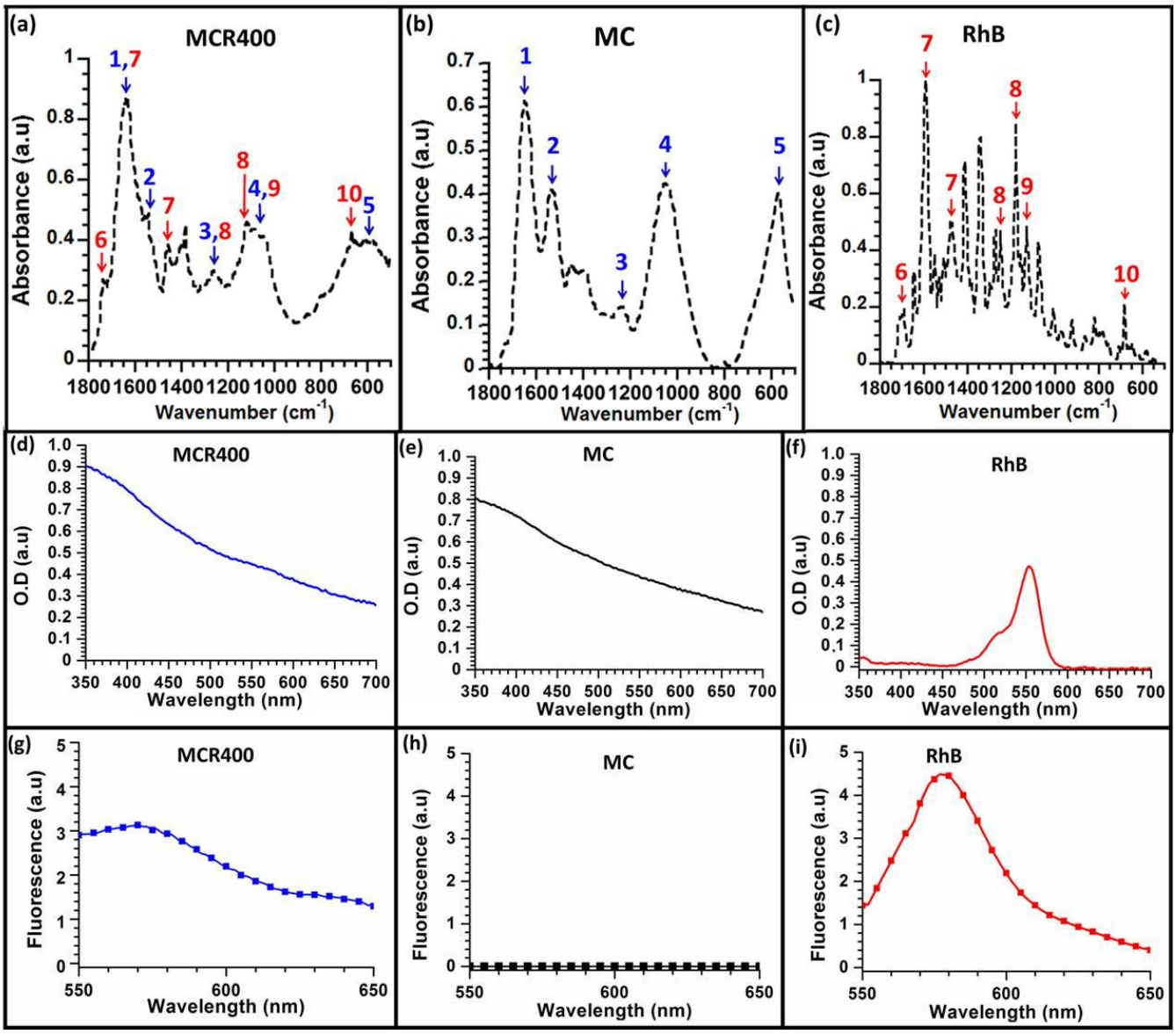
(a)
MCR400
Absorbance (a.u)
Wavenumber (cm-1)
1,7
2
7
6
3,8
8
4,9
10
5
(b)
MC
Absorbance (a.u)
Wavenumber (cm-1)
1
2
3
4
5
(c)
RhB
Absorbance (a.u)
Wavenumber (cm-1)
7
8
7
8
9
6
10
(d)
MCR400
O.D (a.u)
Wavelength (nm)
(e)
MC
O.D (a.u)
Wavelength (nm)
(f)
RhB
O.D (a.u)
Wavelength (nm)
(g)
MCR400
Fluorescence (a.u)
Wavelength (nm)
(h)
MC
Fluorescence (a.u)
Wavelength (nm)
(i)
RhB
Fluorescence (a.u)
Wavelength (nm)

Figure 3

721

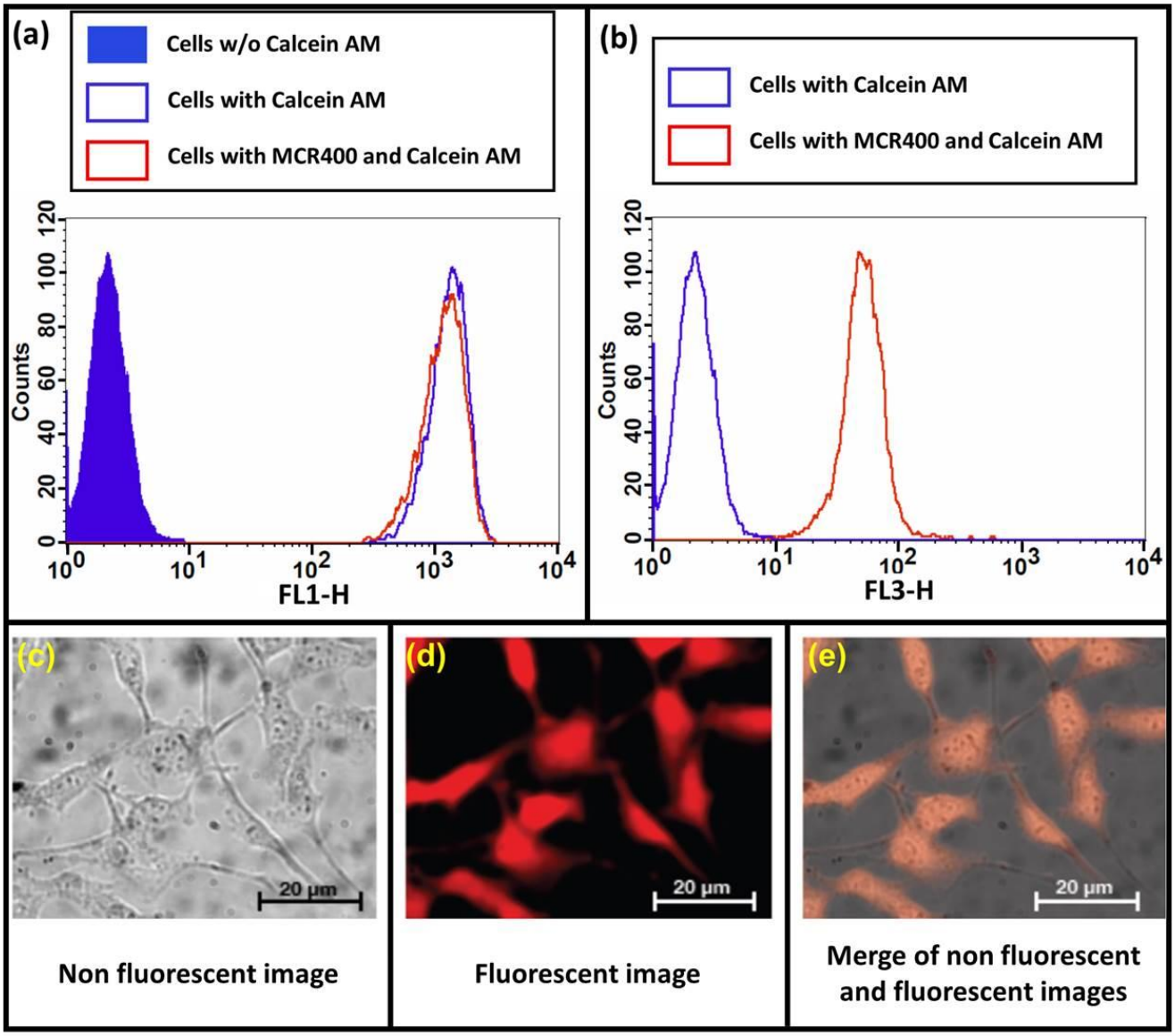
(a)
Cells w/o Calcein AM
Cells with Calcein AM
Cells with MCR400 and Calcein AM
Counts
FL1-H
(b)
Cells with Calcein AM
Cells with MCR400 and Calcein AM
Counts
FL3-H
(c)
20 µm
Non fluorescent image
(d)
20 µm
Fluorescent image
(e)
20 µm
Merge of non fluorescent and fluorescent images

Figure 4

722

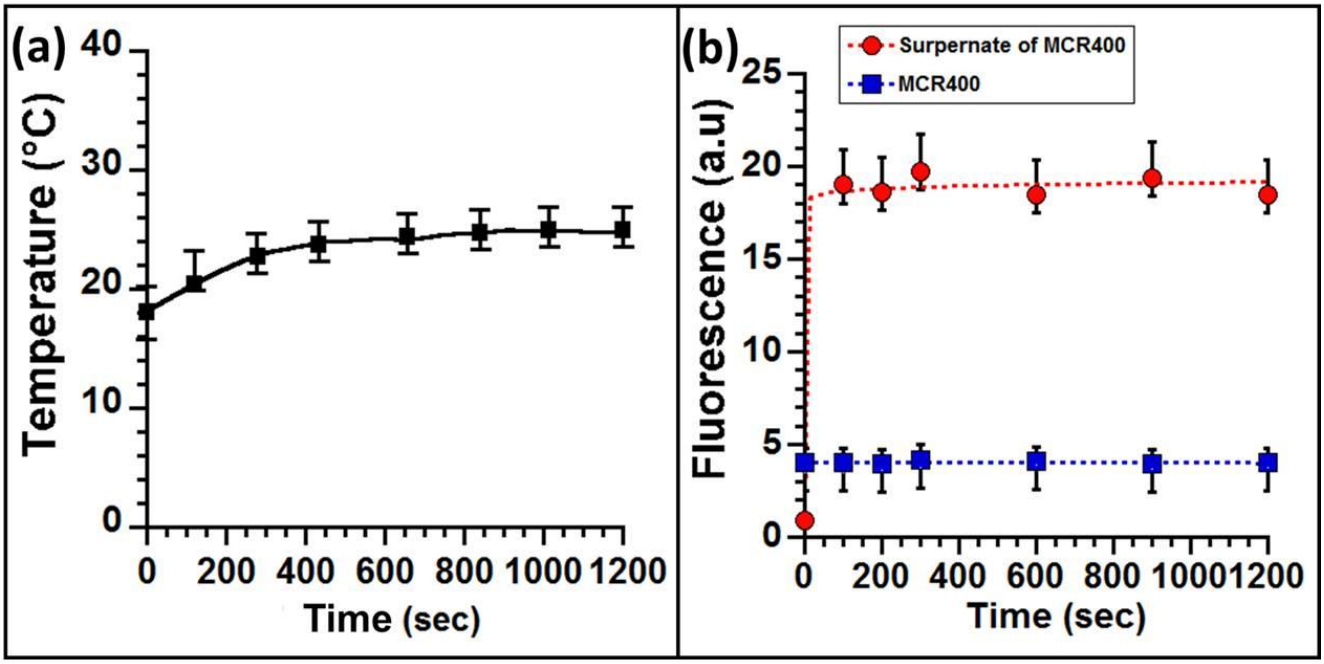
(a)
Temperature (°C)
0
10
20
30
40
0
200
400
600
800
1000
1200
Time (sec)
(b)
Fluorescence (a.u)
0
5
10
15
20
25
Surpernate of MCR400
MCR400
0
200
400
600
800
1000
1200
Time (sec)

Figure 5

723

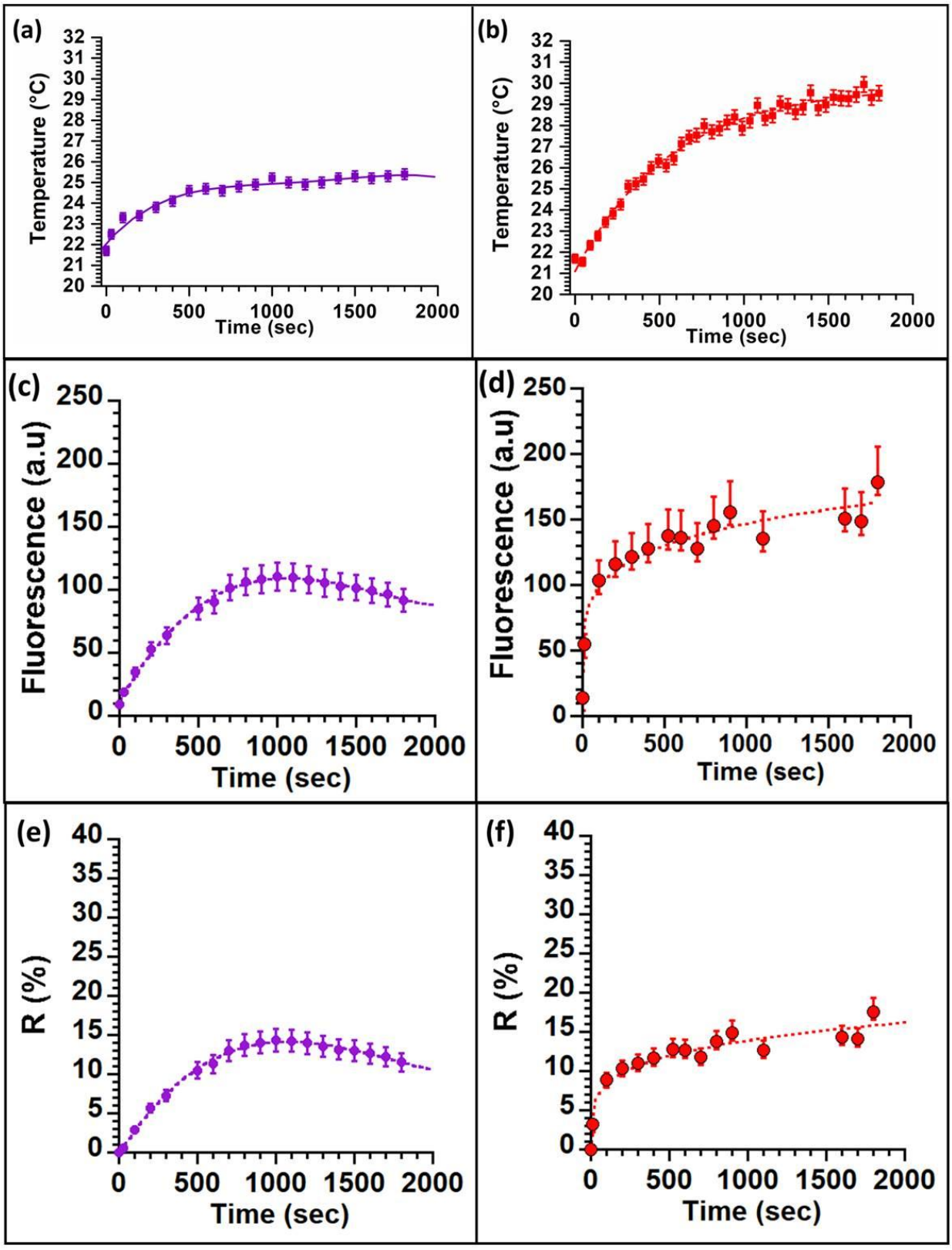
(a)
Temperature (°C)
Time (sec)
(b)
Temperature (°C)
Time (sec)
(c)
Fluorescence (a.u)
Time (sec)
(d)
Fluorescence (a.u)
Time (sec)
(e)
R (%)
Time (sec)
(f)
R (%)
Time (sec)

Figure 6

724

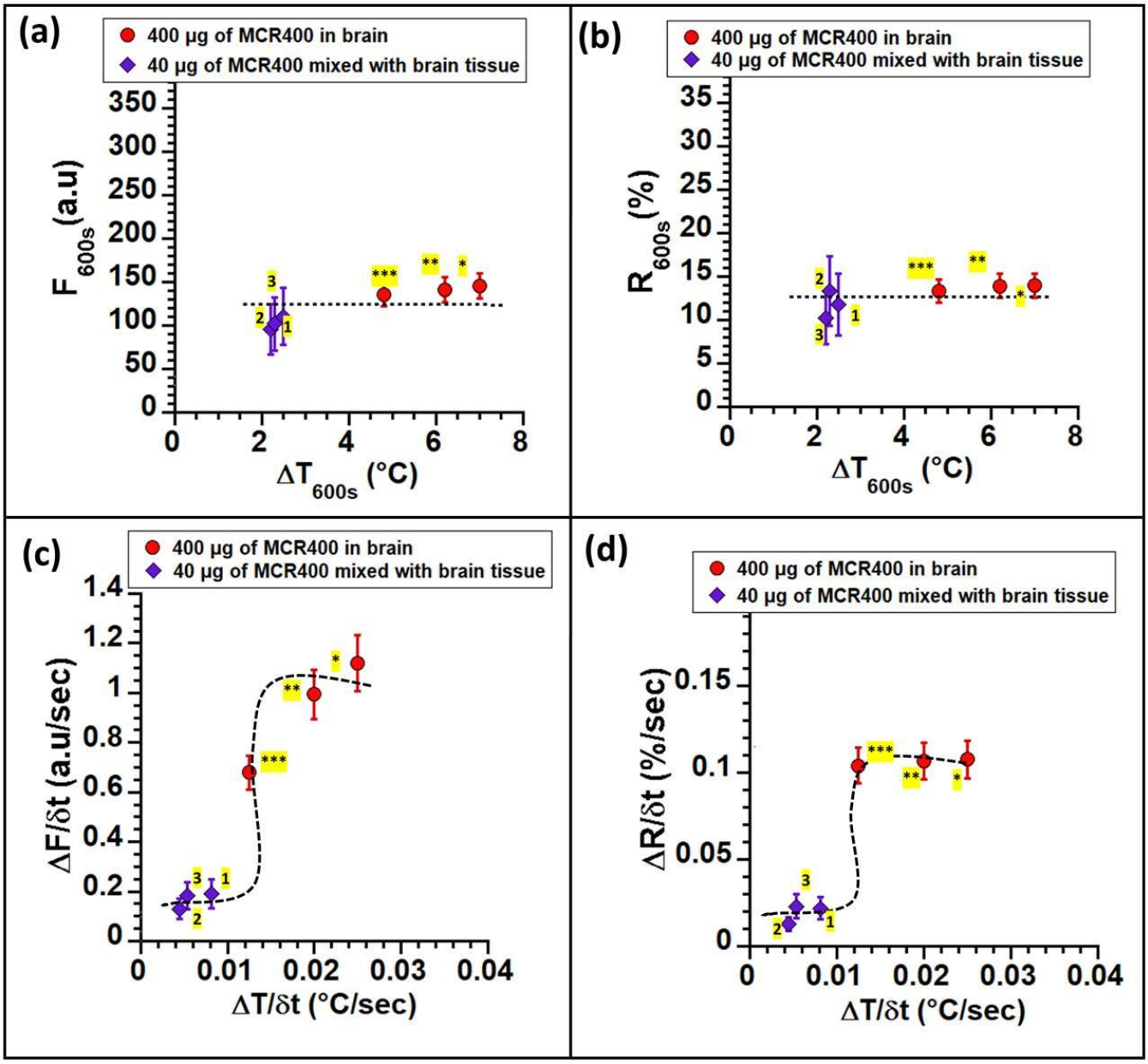
(a)
400 µg of MCR400 in brain
40 µg of MCR400 mixed with brain tissue
F600s (a.u)
ΔT600s (°C)
(b)
400 µg of MCR400 in brain
40 µg of MCR400 mixed with brain tissue
R600s (%)
ΔT600s (°C)
(c)
400 µg of MCR400 in brain
40 µg of MCR400 mixed with brain tissue
ΔF/δt (a.u/sec)
ΔT/δt (°C/sec)
(d)
400 µg of MCR400 in brain
40 µg of MCR400 mixed with brain tissue
ΔR/δt (%/sec)
ΔT/δt (°C/sec)

Figure 7

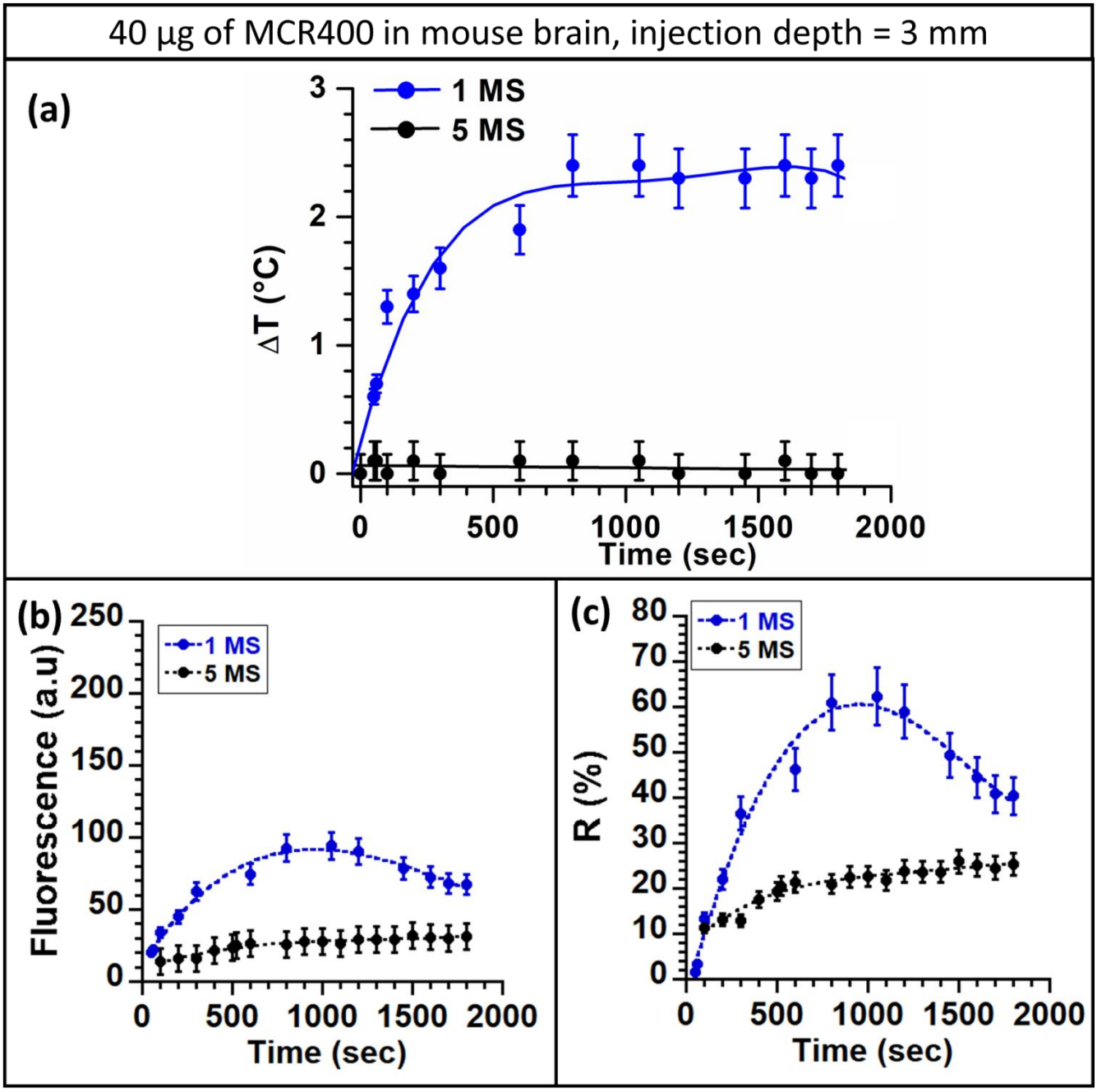
40 μg of MCR400 in mouse brain, injection depth = 3 mm
(a)
1 MS
5 MS
ΔT (°C)
Time (sec)
(b)
Fluorescence (a.u)
1 MS
5 MS
Time (sec)
(c)
R (%)
1 MS
5 MS
Time (sec)

Figure 8

726

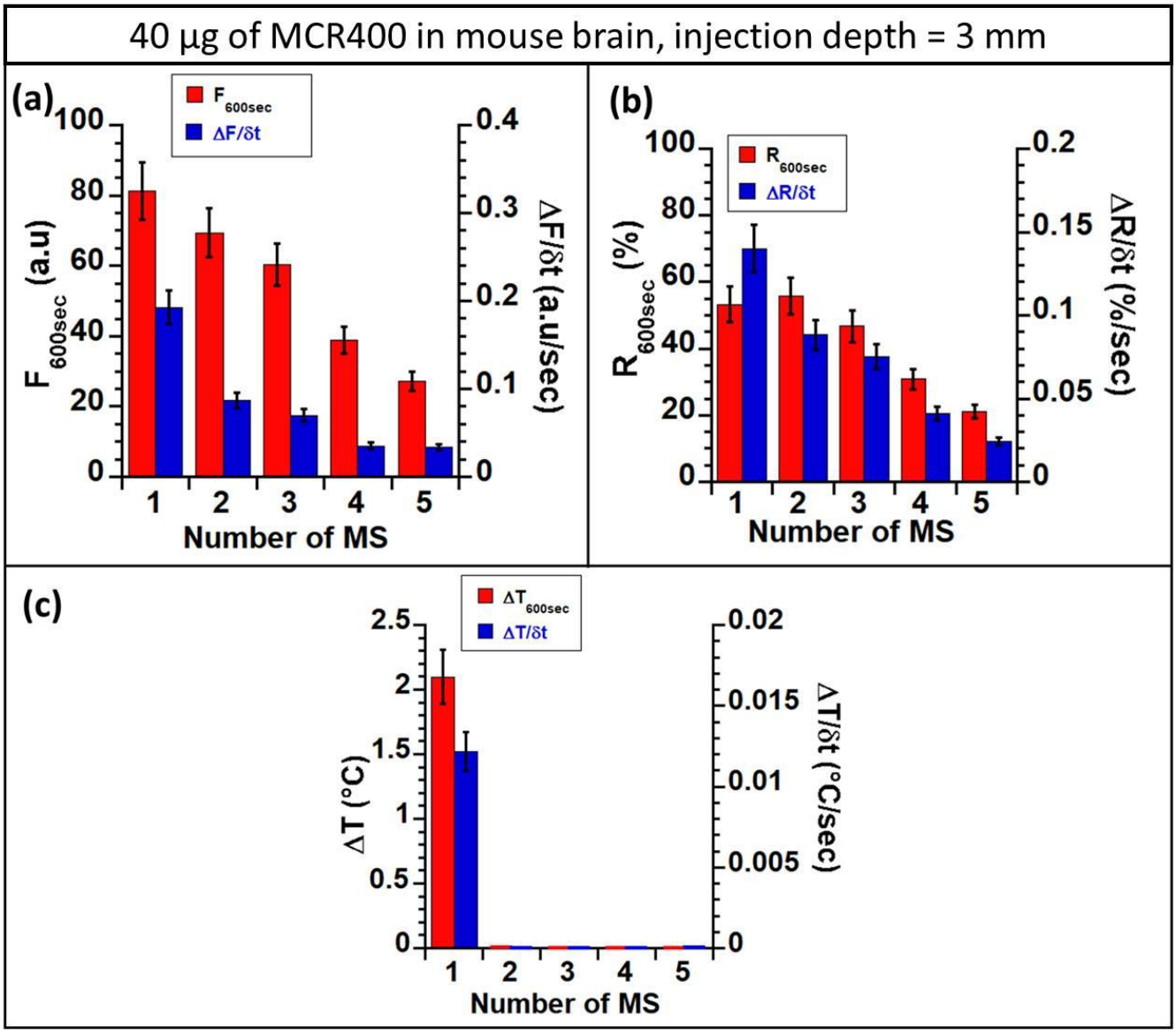
40 µg of MCR400 in mouse brain, injection depth = 3 mm
(a)
F600sec
ΔF/δt
F600sec (a.u)
ΔF/δt (a.u/sec)
Number of MS
(b)
R600sec
ΔR/δt
R600sec (%)
ΔR/δt (%/sec)
Number of MS
(c)
ΔT600sec
ΔT/δt
ΔT (°C)
ΔT/δt (°C/sec)
Number of MS

Figure 9

727